

# Probing Excited State Dynamics of Copper Complexes and Investigating Catalysis via Single Electron Transfer

Vidhyalakshmi S.

(MS14153)

*A dissertation submitted for the partial fulfilment of  
BS-MS dual degree in Science.*



Indian Institute of Science Education and Research Mohali

April 2019

# Certificate of Examination

This is to certify that the dissertation titled “Probing Excited State Dynamics of Copper Complexes and Investigating Catalysis via Single Electron Transfer” submitted by Ms Vidhyalakshmi S. (Reg. No. MS14153) for the partial fulfilment of BS-MS dual degree programme of the Institute, has been examined by the thesis committee duly appointed by the Institute. The committee finds the work done by the candidate satisfactory and recommends that the report be accepted.

Dr. Sanjay Singh

Dr. Angshuman Roy Choudhury

Dr. Debashis Adhikari

(Supervisor)

# Declaration

The work presented in this dissertation has been carried out by me under the guidance of Dr. Debashis Adhikari at the Indian Institute of Science Education and Research Mohali. This work has not been submitted in part or in full for a degree, a diploma, or a fellowship to any other university or institute. Whenever contributions of others are involved, every effort is made to indicate this clearly, with due acknowledgement of collaborative research and discussions. This thesis is a bonafide record of original work done by me and all sources listed within have been detailed in the bibliography.

Vidhyalakshmi S.

April 26, 2019

In my capacity as the supervisor of the candidate's project work, I certify that the above statements by the candidate are true to the best of my knowledge.

Dr. Debashis Adhikari.

(Supervisor)

# Acknowledgement

I would like to dedicate this thesis to my Parents for supporting me throughout these five years of my undergraduate studies. My sincere thanks to my sister Vijayalakshmi for being a wonderful companion.

My sincere thanks to the Department of Science and Technology, Government of India for the INSPIRE funding of 5 years. My heartfelt gratitude to IISER-Mohali for providing a highly intellectually stimulating and competitive environment for my undergraduate studies.

I would like to sincerely thank my thesis supervisor Dr. Debashis Adhikari for being a huge moral support and constant motivation throughout this one year of my master's thesis. My special thanks to him for believing in my capability and giving me immense confidence that kept me enthusiastic throughout the year. I would also like to express my gratitude to my committee members Dr. Sanjay Singh and Dr. Angshuman Roy Choudhary for their useful suggestions and encouragement. My heartfelt thanks to Kirti Singh for helping me with the entire laboratory work and for all the affection and care that served as a huge morale booster.

I would also like to thank my friends Vinita Kumari, Aswathy P.R and Budaraju Sasank for their invaluable support and confidence in me this entire year. My sincere thanks to Jeiyendira Pradeep .D and Swetha Srinivasan for being an amazing inspiration and an emotional support throughout these five years.

Vidhyalakshmi S.

# List of Figures

Figure 1.1 Mechanism of  $\text{Ru}(\text{bpy})_2^{2+}$  action during photosensitization.

Figure 1.2 UV-Vis NIR spectrum of  $10^{-5}$  M solution of **C1** in dry DCM at RT.

Figure 1.3 Solvatochromism of the excited state of  $10^{-5}$  M solutions of **C1** ( $\lambda_{\text{exc}}=385\text{nm}$ )

Figure 1.4 Photoluminescence decay of **C1** and **C2** in THF ( $\lambda_{\text{exc.}} = 385\text{nm}$  and  $\lambda_{\text{pl}}=410\text{nm.}$ )

Figure 1.5 Photoluminescence decay of **C1(a), (b) and (c)** ( $\lambda_{\text{exc}} = 385\text{nm}$  and  $\lambda_{\text{pl}}= 410\text{nm.}$ )

Figure 1.6 UV-Vis NIR spectra of  $10^{-5}$  M solutions of **C1** and **C2** in DCM at RT.

Figure 1.7 Optimized first excited state geometry of **C'**

Figure 1.8 Optimized ground state geometry of **C'**

Figure 1.9 UV-Vis NIR spectrum of **C3** in dry DCM at RT

Figure 1.10 Emission spectra of **C3** excited at  $\lambda=450\text{nm}$  at RT.

Figure 1.11 Emission spectra of **C3** at  $\lambda=45\text{nm}$  at RT

Figure 1.12 Temperature dependent Photoluminescence spectra of **C3** in Toluene

Figure 1.13 Temperature dependent Photoluminescence spectra of **C3** in MeCN

Figure 1.14 Photoluminescence decay of  $10^{-5}$  M solution of **C3** in a) THF b) MeCN

c) Toluene d) DCM ( $\lambda_{\text{exc}} = 385 \text{ nm}$   $\lambda_{\text{em}} = 450 \text{ nm}$ )

Figure 2.1  $\text{S}_{\text{RN}}1$  Mechanistic pathway defining SET

Figure 2.2 Hypothesis of site selective C-H activation mediated by SET

Figure 2.3 The HRMS spectrum of **C4** indicates the monomeric nature in solution

Figure 2.4 UV-Vis absorption spectrum of  $10^{-5}$  M solution of **C4** in DCM at RT

Figure 2.5 Dual parameter Hammett fit indicating the dominant radical effect of

the substituent.

Figure 2.6 Proposed mechanism for SET mediated Hydrosilylation

# List of Photographs

Picture 1.1 (a) The ligand and C3 in visible light (b) The ligand and C3 visualized at 365nm

Picture 1.2 (a) Crystalline C3 in visible light (b) Crystalline C3 visualized at 365nm

# List of Tables

Table 2.1 Optimization conditions for the reaction by varying reaction temperature

Table 2.2 Summary of Results and Analysis

Table 2.3 Summary of substrate scope establishing generality of the aziridination reaction

Table 2.4 The Diverse substrate scope establishing the generality of Hydrosilylation. .



# List of Schemes

Scheme 1.1 . Scheme for synthesis of BIAN

Scheme 1.2 . Scheme for synthesis of D2

Scheme 1.3 . Synthetic scheme for donor-acceptor complexes

Scheme 2.1 . Synthesis of ligand PLY

Scheme 2.2 . Synthesis of the catalyst Ni(Ply)<sub>2</sub>

Scheme 2.3 . Synthesis of catalyst C4

Scheme 2.4 . Synthetic procedure of PhInTs

Scheme 2.5 . Reaction scheme for Aziridination

Scheme 2.6 . Reaction scheme for Aziridination

Scheme 2.7 . Reaction scheme for hydrosilylation

Scheme 2.8 . Competitive experiments to establish Hammett correlation

# List of Notations

|                 |                                    |
|-----------------|------------------------------------|
| aq.             | Aqueous                            |
| Ar              | Aryl                               |
| Bu              | Butyl                              |
| d               | Doublet                            |
| DCM             | Dichloromethane                    |
| dd              | Doublet Of Doublet                 |
| eq.             | Equation                           |
| equiv.          | Equivalent                         |
| Fig.            | Figure                             |
| HOMO            | Highest Occupied Molecular Orbital |
| <sup>i</sup> Pr | Isopropyl                          |
| LUMO            | Lowest Occupied Molecular Orbital  |
| m               | Multiplet                          |
| Me              | Methyl                             |
| MeCN            | Acetonitrile                       |
| mg              | Milligram                          |
| ml              | Millilitres                        |
| mL              | Millilitre                         |
| mmol            | Millimole                          |
| NacNac          | 1,3-Diketimines                    |
| NIR             | Near Infrared Region               |
| NMR             | Nuclear Magnetic Resonance         |
| o               | Degree                             |
| Ph              | Phenyl                             |
| Ppm             | Parts Per Million                  |
| q               | Quartet                            |
| rt              | Room Temperature                   |
| s               | Singlet                            |
| t               | Triplet                            |
| tBu             | Tert-Butyl                         |
| td              | Triplet Of Doublets                |

|               |                           |
|---------------|---------------------------|
| TLC           | Thin Layer Chromatography |
| UV            | Ultra-Violet              |
| v/v           | Volume By Volume          |
| Vis           | Visible                   |
| $\delta$      | Chemical Shift            |
| $\mu$         | Micro                     |
| $\mu\text{L}$ | Micro-Litre               |

# Contents

|   |             |
|---|-------------|
| <b>List of Figures .....</b>  | <b>v</b>    |
| <b>List of Photographs.....</b>   | <b>vi</b>   |
| <b>List of Tables List of Schemes.....</b>  | <b>vii</b>  |
| <b>List of Schemes.....</b>   | <b>viii</b> |
| <b>List of Notations.....</b>   | <b>ix</b>   |
| <b>Abstract.....</b>  | <b>xiii</b> |
| <b>Chapter 1.....</b>   | <b>1</b>    |
| <b>Probing excited state dynamics of Base Metal Complexes</b>                     |             |
| 1.1 Introduction.....   | 1           |
| 1.2 Experimental Section.....   | 5           |
| 1.2.1 Chemicals.....  | 5           |
| 1.2.2 Spectroscopic measurements.....   | 5           |
| 1.2.3 Synthesis.....  | 6           |
| 1.3 Results and Discussion.....   | 8           |
| 1.4 Summary.....  | 18          |
| <b>Chapter 2.....</b>   | <b>19</b>   |
| <b>Investigating Single Electron transfer (SET) mediated Base metal catalysis</b> |             |
| 2.1 Introduction.....   | 20          |
| 2.2 Experimental Section.....   | 21          |
| 2.2.1 Chemicals.....  | 21          |
| 2.2.2 Synthesis.....  | 21          |

|                                 |           |
|---------------------------------|-----------|
| 2.2.3 Catalysis .....           | 22        |
| 2.3 Results and Discussion..... | 24        |
| 2.4 Summary.....                | 32        |
| <b>Bibliography.....</b>        | <b>33</b> |
| <b>Appendix.....</b>            | <b>36</b> |

# Abstract

The major theme of the work presented in this dissertation is to develop an understanding of the basic processes that govern the excited state of transition metal complexes and to shed an insight into the mechanism of single electron transfer as a means of driving catalysis. Charge transfer states and unique photophysical characteristics exhibited by transition metal complexes have been probed to develop a strong foothold on the driving processes of photosensitization. The excited state dynamics coupled with the lifetime of homoleptic and heteroleptic base metal systems has been thoroughly investigated with substantial experimental and computational aids to arrive at appropriate strategies with the intent of developing an effective and cost efficient photosensitizer to replace the conventional noble metal photosensitizers. In the other part of the thesis, base metal assisted catalysis of two industrially significant reactions have been established. The role of redox active ligands to serve as an electron reservoir facilitating single electron transfer catalysis has been investigated.



# Chapter 1

## Probing excited state dynamics of Base Metal Complexes

---

### 1.1 INTRODUCTION

#### Charge Transfer states in Metal Complexes:

The electronic spectrum of a metal ligand system is often attributed to three distinct type of transitions namely:

- a) Transitions that occur between the electronic levels centered on the metal (d-d)
- b) Transitions that occur between the electronic levels centered on the ligand ( $\pi$ - $\pi^*$ )
- c) Transitions that occur between the electronic levels from metal to ligand or vice-versa

The third type of transition often known as charge transfer is primarily responsible for the intense color of the solution of metal complexes with no d-electrons. The transitions may correspond to different energies but what is of practical significance are those transitions that correspond to the visible light region of the electromagnetic spectrum. The HOMO-LUMO gap could be qualitatively ascribed to a molecule's ionization potential. Hence, the molecule that is easily oxidizable has a high energy HOMO and conversely, a molecule that is easily reduced has a low lying LUMO. So, in a conventional sense, in a metal ligand system with the metal bound to an easily oxidizable and a easily reducible ligand on either side, the ligand that has a high ionization potential tends to give an electron easily is called the DONOR and similarly, the ligand that is readily reduced has the tendency to accept an electron easily and is called an ACCEPTOR. If the metal is readily oxidizable or readily reducible, there are three types of probable transitions depending on the energy separation between the corresponding levels of the metal and the ligands namely,

- a) Ligand to Ligand Charge Transfer (LLCT).
- b) Metal to Ligand Charge Transfer (MLCT).
- c) Ligand to Metal Charge Transfer (LMCT).



### **Ligand to Ligand Charge Transfer (LLCT):**

The Ligand to ligand charge transfer is usually facilitated by a metal ligand system with an electron rich donor ligand and an electron deficient acceptor ligand with a special emphasis on the design such that the HOMO and the LUMO are centered on the donor and acceptor ligand respectively. This electronic configuration necessitates that the metal d orbitals be energetically removed from the ligand-based frontier orbitals to avoid low-energy, metal-based excited states. A coplanar arrangement of the ligands on either side of the transition metal further enhances the probability of LLCT.

### **Ligand to Metal Charge Transfer (LMCT):**

If in a system where the HOMO is predominantly centered on the readily oxidizable ligand and the LUMO centered on the easily reducible metal the ligand is bound to, transition happens from the ligand to the metal. In a donor-acceptor system, this generally happens when the metal LUMO is slightly higher than the acceptor LUMO facilitating LMCT rather than LLCT. There are no known specific geometric restrictions on LMCT. These transitions are pronounced and often result in good chromophores.

### **Metal to Ligand Charge Transfer (MLCT)**

The transition that occurs from a filled HOMO centered on the metal to an easily reducible ligand LUMO is what constitutes a metal to ligand charge transfer. The charge transfer band is expected to move to lower energy as the oxidation state of the metal decreases and as the ligand becomes more electronegative, and to move to higher energies as the coordination number decreases<sup>1</sup>. Ligand design should be such that it would have empty orbitals of appropriate energy and symmetry. These transitions generally correspond to the high energy region and are well pronounced. These characteristics of MLCT play a crucial role in designing dyes and photosensitizers with good quantum efficiency.

### **Photosensitization**

The phenomenon by which any molecule induces a chemical change in another molecule via a photochemical process is commonly termed as photosensitization. Photosensitizers are often an integral part of photodynamic therapy<sup>2</sup>, solar energy conversion<sup>3</sup> among other diverse range of applications. The significant factors that characterize a good photosensitizer include a long lived excited state, extensive  $\pi$  delocalization to facilitate

absorption in the visible region. Most of the well-established and conventional photosensitizers designed and tested in the past few decades includes the use of noble metal bound to an acceptor ligand with a low lying  $\pi^*$  orbital and is primarily based on the MLCT of these complexes.<sup>4</sup> So, there is a pressing need to develop a cheaper and more effective version of these photosensitizers for wider and an effective utilisation<sup>5</sup>. 3dtransition metal substitutes of these noble metal photosensitizers are highly desirable in this perspective.

### [Ru(bpy)<sup>3</sup>] : The Blockbuster Chromophore

Ruthenium when bound to bipyridine ligand absorbs strongly at 452nm characterized as the MLCT transition. The transition has been characterized to be from Ru ( $t_{2g}$ ) to the  $\pi^*$  of bipyridine ligand<sup>6</sup>. With an excited state lifetime in the order of microseconds, the molecule has been well exploited as an excited state reductant in a number of solar energy conversion systems. Some of the inherent properties of this complex limit its utility which includes the lack of tunability of the HOMO and LUMO with the HOMO being centered on the metal rendering it difficult to be tuned. Further Ruthenium being an expensive metal makes it all the more necessary to look for a more commercially viable option with a cheaper base metal MLCT system.

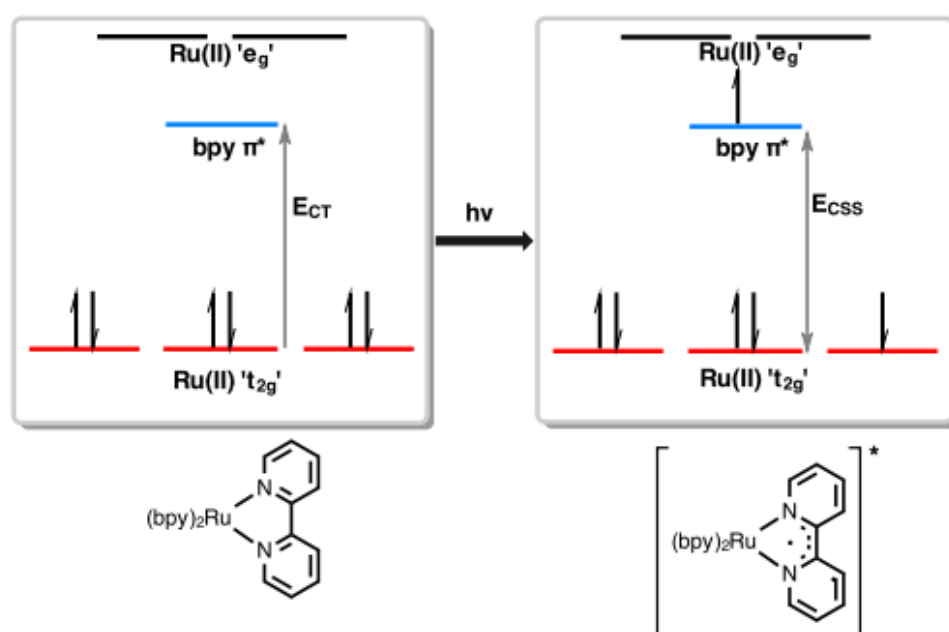


Figure 1.1 Mechanism of Ru(bpy)<sub>2</sub><sup>2+</sup> action during photosensitization.

## Charge transfer states in base –metal complexes

Base metals bound to ligands with low lying  $\pi^*$  orbitals generally possess characteristic charge transfer states. Understanding the dynamics of the excited state of these complexes sheds light on the photosensitization behaviour by the complexes. There have been literature reports on LLCT in heteroleptic base-metal complexes with a donor and an acceptor ligand combination<sup>7</sup>. Emphasis has been laid on the flexibility of tuning HOMO-LUMO which are ligand centric. Also, there have been numerous reports on the MLCT state exhibited by homoleptic metal complexes.<sup>8</sup> Some of the widely explored metal complexes include Nickel based complexes<sup>9</sup> as well as Copper based homoleptic complexes.<sup>10</sup> Bipyridine as the acceptor has been widely exploited. Of late, other ligands have been explored as acceptors and have been proved to be as efficient as bipyridine. The aim of this work is to explore the charge transfer states in heteroleptic Copper (I) complexes which haven't been explored much in the literature. The concept of donor influence in tuning the MLCT from the metal centric HOMO to the acceptor LUMO has been explored. BIAN as an acceptor has been used along with investigations on the effect of substitutions on the charge transfer states. The  $\pi$ - $\pi^*$  transitions in the ligand backbone often called the intra ligand charge transfer band (ILCT) and the implied photophysical characteristics has been investigated. The excited state lifetimes have been measured to substantiate the potential candidacy for photosensitization. An attempt to establish this as a model system for other base metal Heteroleptic complexes has been made. The second system that has been extensively investigated is a homoleptic Zinc (II) complex bound to the NacNac ligand. The ligand has been explored as an acceptor owing to the low lying LUMO. The photophysical properties of this complex has been investigated extensively to understand the underlying mechanisms of the unique chromophoric behaviour of this complex. Salient features of this design include easy and convenient synthesis, heavy conjugation on the ligand backbone and an electron rich metal centre. The solid state luminescence behaviour has been investigated to test the idea of its potential to be fabricated as a light emitting device. The unique chromophoric behaviour exhibited by these systems led to interesting conclusions on their potential applications.

## 1.2 EXPERIMENTAL SECTION

### General Information:

#### 1.2.1 Chemicals

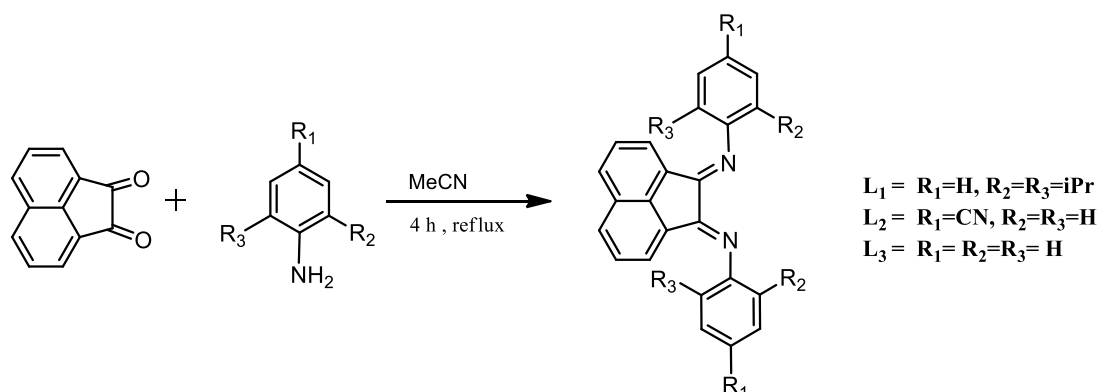
All the reagents and solvents used for synthesis were laboratory grade purchased from AVRA chemicals, Sigma Aldrich and TCI chemicals. The solvents THF and Toluene used for synthesis were dried by standard distillation over Sodium benzophenone. The solvents used for the spectroscopic measurements were analytical grade solvents purchased from Sigma Aldrich and used without further purification. The reaction progress during synthesis was monitored by thin layer chromatography (Sigma Aldrich) and visualized under UV light (254 nm).

#### 1.2.2 Spectroscopic Measurements

$^1\text{H}$  and  $^{13}\text{C}$  NMR spectra were recorded in BrukerBiospin 400MHz spectrometer with Tetra methyl Silane as standard at room temperature. The solvent used for measurement is  $\text{CDCl}_3$  for all the products. UV-Vis Spectroscopic measurements were recorded on PerkinElmer LAMBDA 365 UV/Vis-NIR spectrophotometer using a 1mm path length quartz cuvette at room temperature. Fluorescence spectroscopy measurements were recorded in a HORIBA scientific FLUOROMAX spectrophotometer using a 10mm cuvette. Standard analysis software .was used for analysis and visualization of the spectra. Lifetime measurements were recorded using the Time Correlated Single Photon Counting technique with the help of Horiba Scientific spectrophotometric setup with lasers of different wavelengths (385 nm, 415 nm) . The prompt was a 10% Ludox solution.

## 1.2.3 Synthesis

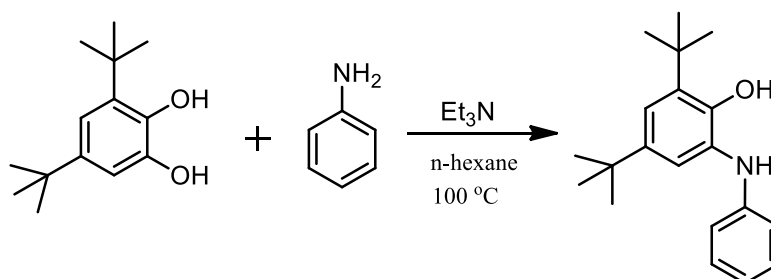
### 1.2.3.1 Procedure for the Synthesis of 1,2bis [(phenyl imino)]-acenaphthene (BIAN)



Scheme 1.1 Scheme of synthesis of BIAN

Aniline (6.21 mM) was treated with of Zinc chloride (8.1 mM ) in Acetic acid (10ml) in a vacuum dried two neck round bottom flask. The reaction mixture was refluxed in Acetic acid for 45 minutes. The resulting bright yellow coloured precipitate was filtered and suspended in a hot solution of Acetic acid again for 15 minutes and filtered. The filtered precipitate was well dried and extracted in a 50:50 mixture of DCM and Potassium Oxalate solution. The organic layer was separated and passed through a thin layer of anhydrous Magnesium Sulphate. The solvent was removed by rotary – evaporation under reduced pressure and the product was obtained as a bright yellow coloured solid. A single spot in the TLC suggested the reaction was complete with no impurities.

### 1.2.3.2 Procedure for the Synthesis of 4,6-Di-tert-butyl-2-(phenyl amino)phenol (D2)

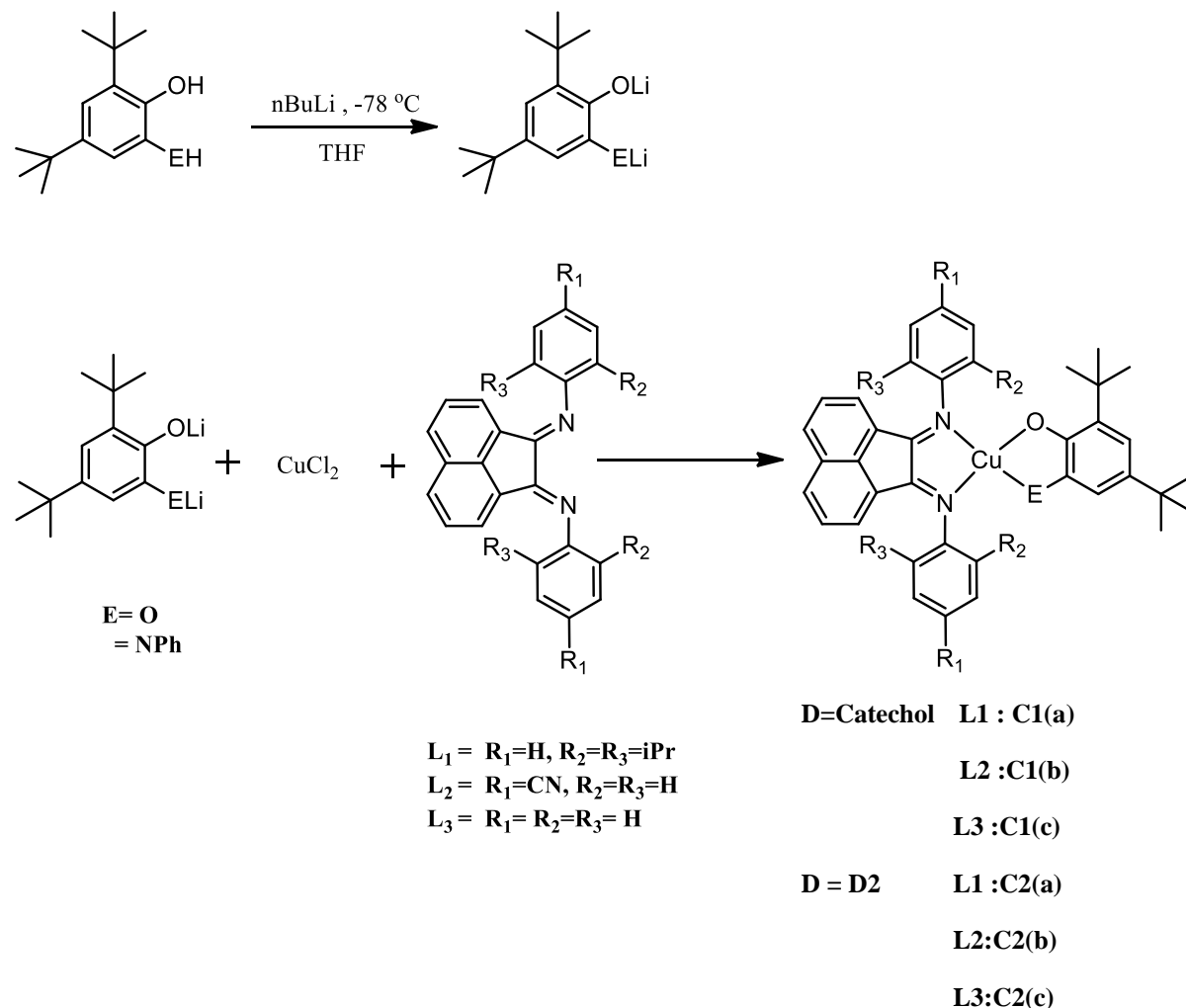


Scheme 1.2. Scheme for synthesis of D2

Aniline (6.21mM) was added to a solution of 3,5 di-tert-butyl catechol in n-Hexane (20 ml). To this reaction mixture Triethylamine (0.12 ml) was added drop wise . The reaction

mixture was refluxed for 5 hours. The suspension was then cooled in ice for 12 hours and filtered. The product was recrystallized in n-hexane as a greyish white solid.

### 1.2.3.3 General Procedure for the synthesis of Donor-Acceptor Complexes.\*



Scheme 1.3. General synthetic scheme for Donor-Acceptor complexes

One molar equivalent of the donor molecules (Catechol / D2) in dry THF was treated with two molar equivalents of n-Butyl Lithium in a dry schlenk flask under Argon atmosphere at -78 °C. The solution was slowly warmed up to RT. This was then treated with one molar equivalent of Copper(I)chloride and one molar equivalent of BIAN under Argon atmosphere. The reaction mixture was stirred overnight at RT. The dark green coloured product was filtered. The product was then dissolved in pure DCM and left at -20 °C overnight. The pure precipitate was filtered and used for further spectroscopic characterization. (\* Synthesis of these complexes has been carried out by Kirti Singh)

## 1.3 RESULTS AND DISCUSSION

All the heteroleptic copper complexes were synthesized by the protocol mentioned in the experimental section.

### 1.3.1 Electronic Properties

All the synthesized copper complexes are highly coloured in both the solid as well as solution state. In the solid state these complexes show an intense green colour and in solution the complexes show a pale green color. The UV-Vis spectra of these complexes show two characteristic bands at  $\lambda_{\text{max}} = 585\text{nm}$  and  $385\text{nm}$  respectively. Copper when bound to catechol as a donor and diimine ligand as acceptor is reported in the literature to show LLCT band with the metal atom adopting a +2 oxidation state. The spectroscopic signature of LLCT bands is solvatochromism in the ground state prominent in the UV-Vis spectrum. Contrary to the literature reports<sup>11</sup>, solvatochromism in the ground state was not prominent for these complexes. Computational analysis showed that Copper when bound to catechol and diimine on either sides, tends to optimize in tetrahedral geometry with the catechol adopting the semi-quinato form and Copper in the more stable +1 oxidation state. Furthermore, the HOMO was found to be centered on the metal and LUMO on the diimine ligand suggesting more probability of a MLCT band. The band at  $585\text{nm}$  is prominent only in the UV-Vis NIR spectra (Figure 2) of the metal complexes and not the ligands and thus was characterized appropriately as (MLCT) band. Similarly, the band centered at  $385\text{nm}$  was characterized as the ILCT band.

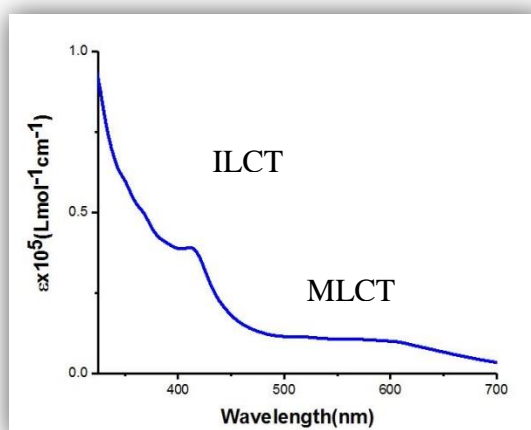


Figure 1.2. UV-Vis NIR spectrum of  $10^{-5}$  M solution of C1 in dry DCM at RT.

### 1.3.2 The ILCT Band

The intra ligand charge transfer band corresponds to the  $\pi$ - $\pi^*$  transition in the heavily delocalized acceptor ligand system. These transitions are known to show a highly polar excited state. The spectroscopic proof for a highly polar excited state is negative solvatochromism (blue shift) in the emission spectra. The ILCT bands of the complexes show strong negative solavatochromism (bathochromic shift) in the excited state with increasing solvent polarity (Figure 3). Solutions of the complexes in three different solvents of varying polarity including highly nonpolar and highly polar solvents showed a conspicuous shift in the  $\lambda_{em}$  towards the higher energy region with increasing solvent polarity upon photo excitation at 385 nm corroborating with the literature results of a highly polar excited state. The spectra have been fitted to a second order binomial for clarity.

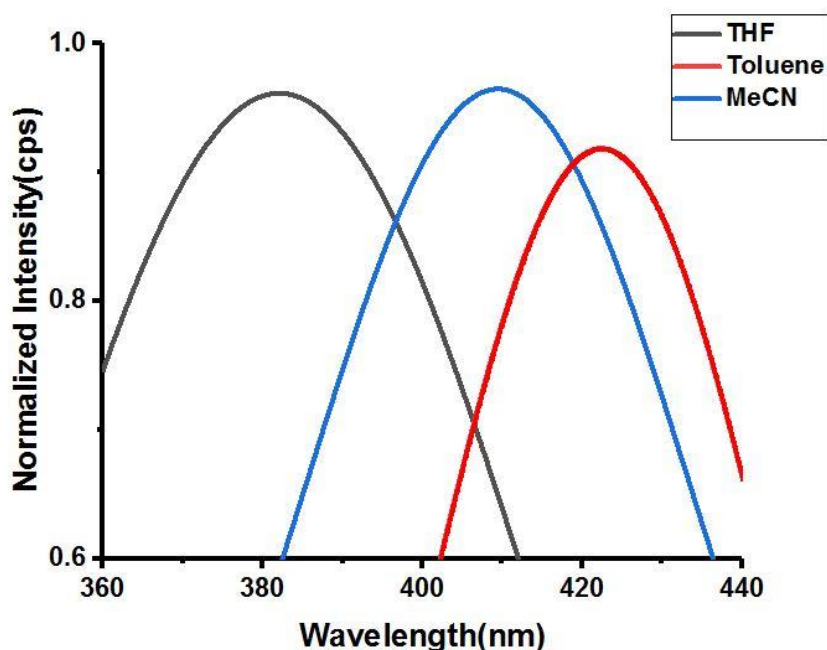


Figure 1.3 Solvatochromism of the excited state of  $10^{-5}$  M solutions of **C1** ( $\lambda_{exc} = 385$  nm)

### 1.3.3 Lifetime of the excited state

Time correlated single photon counting experiments were conducted in an attempt to estimate the lifetime of the excited state. Upon photo excitation with 385nm laser source, a single exponential decay fit with a lifetime of  $1.6 \pm 0.1$  ns was obtained. The lifetimes of the complexes **C1** and **C2** with the same acceptor but different donors were measured in



an attempt to see any possible influence of the donor (Figure 4). But, both the complexes showed a similar lifetime with a difference of 0.1ns with the excited state lifetime of complex **C2** obtained as 1.50ns. Therefore, since the excitation wavelength of 385 nm in the absorption spectrum of the complexes is characterized as the  $\pi$ - $\pi^*$  transition of the acceptor ligand, the lifetimes can be attributed to the excited states corresponding to these transitions. Similarly, the lifetimes of complex **C1** with same donor but different acceptors (different substituted BIAN) were measured (Figure 5) to investigate the effect of donating and withdrawing substituents in the 4' position of the phenyl ring attached to the Nitrogen atom in the ligand. However, there was no significant difference in the lifetime of the excited state of complexes with different acceptors. This suggests that functionalization in some other region of the ligand could have a much more pronounced effect on tuning the  $\pi$ - $\pi^*$  transition of the ligand.

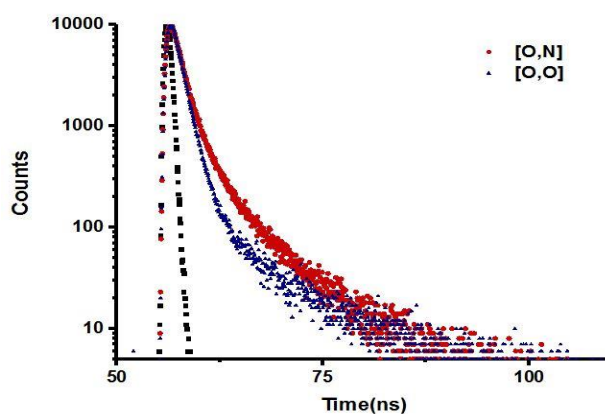


Figure 1.4 Photoluminescence decay of **C1** and **C2** in THF ( $\lambda_{ex}$  385 nm and  $\lambda_{pl}$ = 410 nm.)

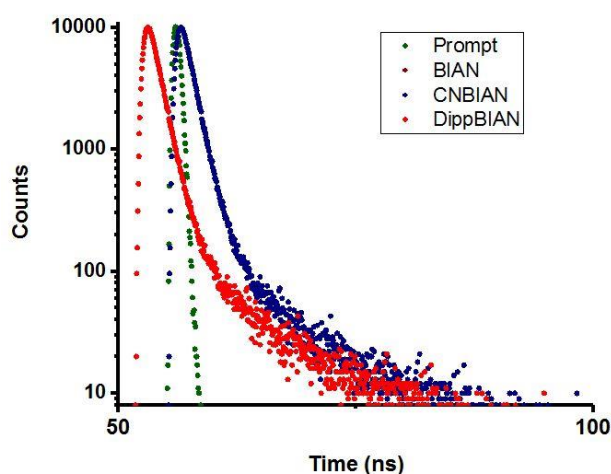


Figure 1.5 Photoluminescence decay of **C1**(a), (b) and (c)( $\lambda_{ex}$  385 nm and  $\lambda_{pl}$ = 410 nm.)

### 1.3.4 Influence of Donor Ligand on MLCT

In general, the tunability of HOMO and LUMO is very limited in MLCT complexes but an attempt was made to investigate any subtle electronic effect of the donor on tuning the MLCT transition from the metal to the acceptor ligand. The UV-Vis NIR spectra of the complexes C1 and C2 showed a clear hypsochromic shift in the MLCT band indicating possible influence of the donor on the charge transfer state. Further attempts to draw decisive conclusions by probing the excited state dynamics of the MLCT state by transient absorption spectroscopy is currently underway.

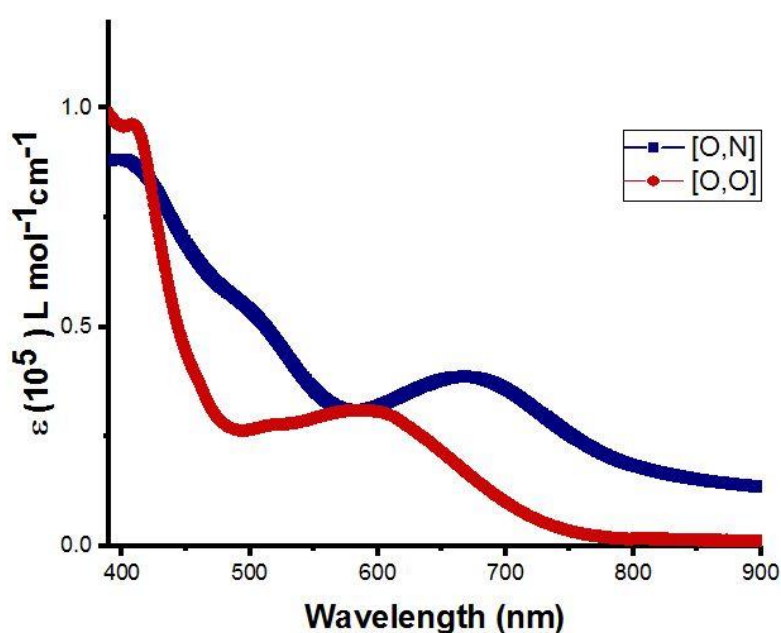


Figure 1.6 UV-Vis NIR spectra of  $10^{-5}$  M solutions of C1 and C2 in DCM at RT.

### 1.3.5 Computational Details

DFT calculation were used to optimize the structure of the molecules in the ground state . The ground state optimized structures for all these molecules revealed optimized tetrahedral geometry which provided further basis for believing the metal centre in the ground state is Copper is the +1 oxidation state. The ground state was revealed to be a doublet and the first excited state a quartet. Further the first excited state of all these molecules showed a fairly square planar structure with resemblance towards Copper (II) centre. This flattening of the excited state is shown to support exciplex formation thereby quenching fluorescence and shortening the excited state lifetime. However, a new molecule (C') has been computationally modeled. Having two Nitrogens with phenyl

substituents bound to the metal centre as the differing donor part shows a more tetrahedral resembling optimized geometry in the first excited state. Such a model system is expected to have a longer lived lifetime and less supportive of exciplex formation.

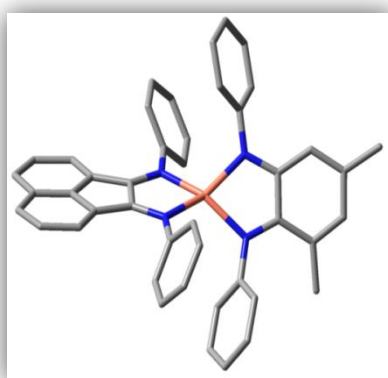
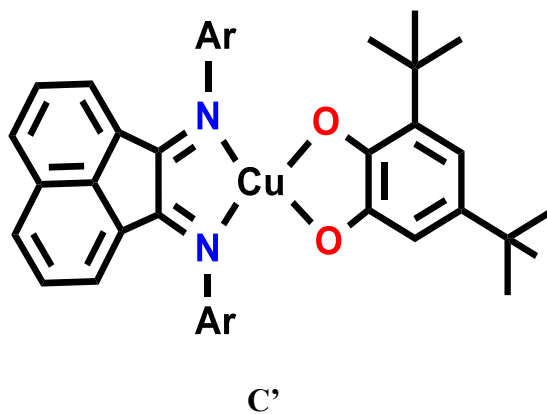


Figure 1.7 Optimised first excited state geometry of C'

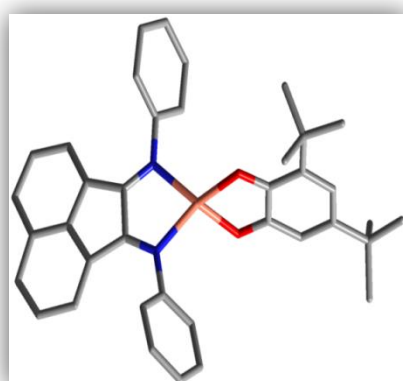
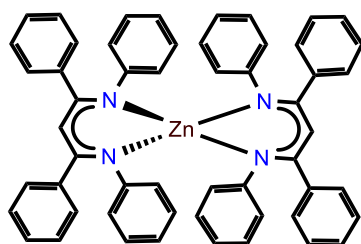


Figure 1.8 Optimised ground state geometry of C'

### 1.3.6 A homoleptic system: $(\text{Zn}(\text{NacNac})_2)^{\text{PhPh}}$

The second category of metal ligand system investigated is a homoleptic base metal system with a Zinc(II) center flanked by N-acetyl acetone with a phenyl substituent ( $\text{NacNac}^{\text{Ph,Ph}}$ ) on both sides. The crystal structure of the molecule revealed a tetrahedral geometry. The electron rich metal center bound to the ligand with a low lying  $\pi^*$  orbital was suggestive of a clear MLCT band. The photo physical characterization of this system revealed interesting properties.



C3

### 1.3.7 Absorption Profile

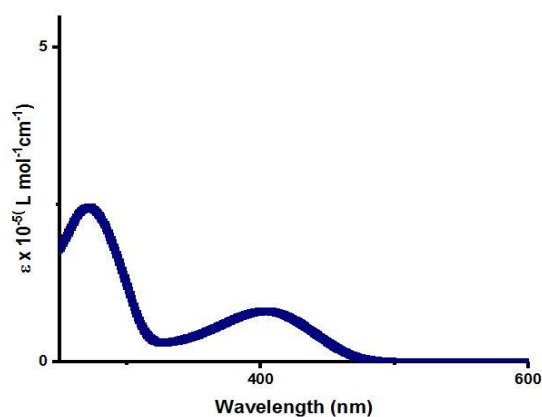
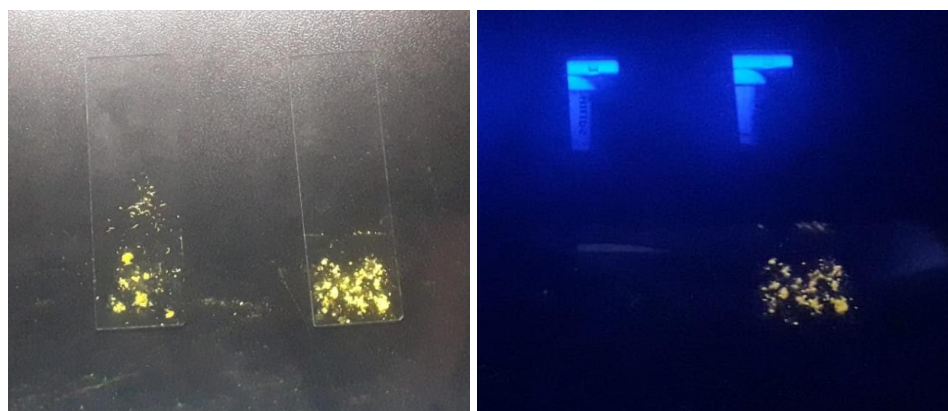


Figure 1.9 UV-Vis NIR spectrum of **C3** in dry DCM at RT.

The complex is bright yellow colored in the solid state and fluorescent yellow in solution. The absorption spectrum shows two prominent bands with maximum wavelengths at 400nm and 350nm. The strong absorbance of the complex in the visible region underlines the significance of this complex as a potential candidate for a good photocatalyst or a molecule for solar energy conversion to drive a chemical change.

### 1.3.8 Solid state Luminescence:

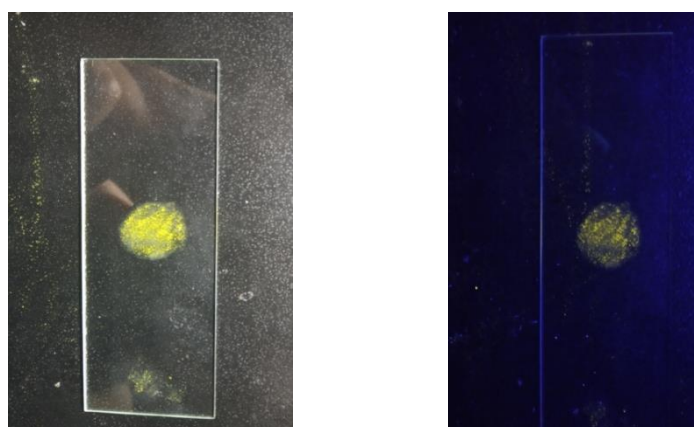
The extensive conjugation in the ligand backbone coupled with a good absorption profile in the visible region led us to probe the fluorescence property of this molecule. The molecule when visualized under the long UV light (365 nm) showed excellent fluorescence in the solid state. This also underlines the significance of the metal complex as the ligand doesn't exhibit solid state luminescence upon visualization under Long UV light (365 nm). C3 exhibits strong luminescence in both amorphous and crystalline phase. This indicates that the crystal packing did not affect the emission characteristics much. Experiments to quantitatively estimate the quantum yields are currently underway. This characteristic property of the complex sheds light on the possibility of fabricating a light emitting device.



(a)

(b)

Picture 1.1 (a) The ligand and C3 in visible light (b) The ligand and C3 visualized at 365nm



Picture 1.2 (a) Crystalline C3 in visible light (b) Crystalline C3 visualized at 365nm

### 1.3.9 Aggregation Induced Emission.

The strong solid state fluorescence of the metal complex led us to probe the mechanism behind the enhanced emission in the solid state. The phenomenon of aggregation induced emission was investigated in two different solvent mixtures. The solvent mixtures included one solvent in which the metal complex was soluble (THF and MeCN) and water in which it is sparingly soluble. As the ratio of Water increased in each of these sets, there was an observed increase in the emission intensity. This phenomenon is in direct contrast to the conventional aggregation caused quenching. Here, aggregation positively restricts intramolecular rotations that often drive non radiative decay and hence efficient emission in a poor solvent is observed.

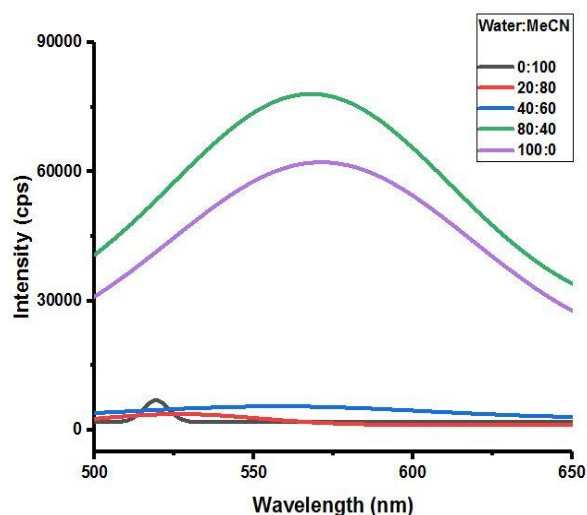


Figure 1.10 Emission spectra of C3 excited at  $\lambda=450$  nm at RT

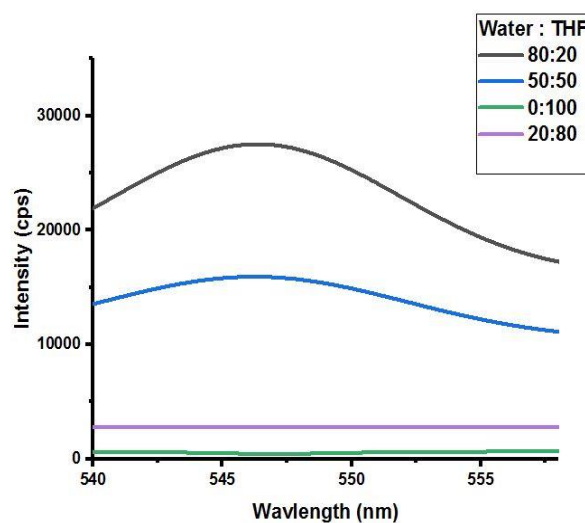


Figure 1.11 Emission spectra of C3 at  $\lambda=450$  nm at RT.

### 1.3.10 Temperature dependence of emission

The emission spectrum of C3 was recorded with gradual change in temperature and an increase in emission intensity with increase in temperature was observed. This corroborates with the fact that increase in temperature provides more energy to populate the excited state and hence an increase in emission intensity. However for the two sets of C3 solutions (in Toluene and MeCN) the observations were different. The emission maxima appeared upon excitation at different wavelengths which essentially meant that two different excited states were getting stabilized in different solvents. There was no significant increase in the emission maxima in response to temperature in case of C3 solution in MeCN. However there is a pronounced increase in emission maxima in response to temperature in solution of C3 in Toluene.

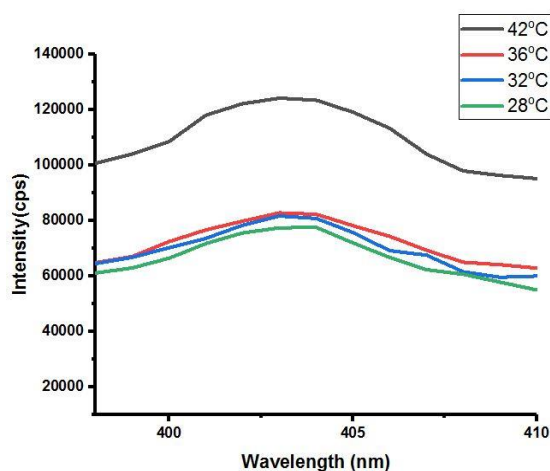


Figure 1.12 Temperature dependent Photoluminescence spectra of C3 in Toluene.

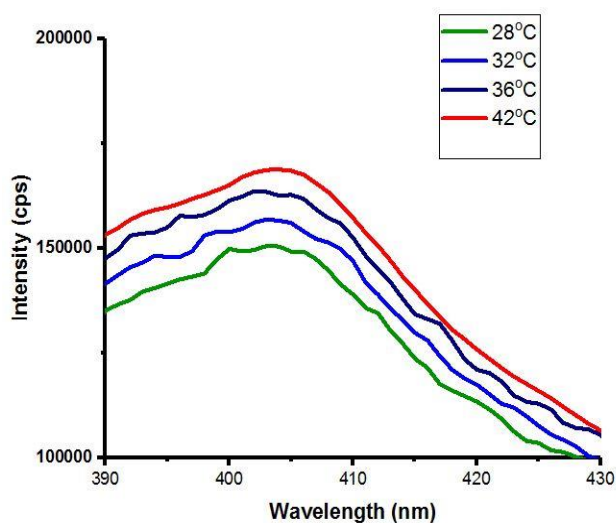


Figure 1.13 Temperature dependent Photoluminescence spectra of C3 in MeCN.

### 1.3.11 Excited state behavior in different solvents

Efforts to investigate photosensitization by C3 are currently underway. In order to establish the reaction conditions, excited state lifetime of C3 in different solvents were measured. It was observed that the lifetime of the excited state upon excitation at  $\lambda=385\text{nm}$  is in the domain of 2-4 ns. The maximum lifetime was observed in DCM ( $\tau = 4.38 \pm 0.01\text{ns}$ ), hence DCM would be chosen as the solvent medium for the photosensitization reaction. The decay profile was similar for all the solvents and the prompt for all measurements was 10% Ludox solution.

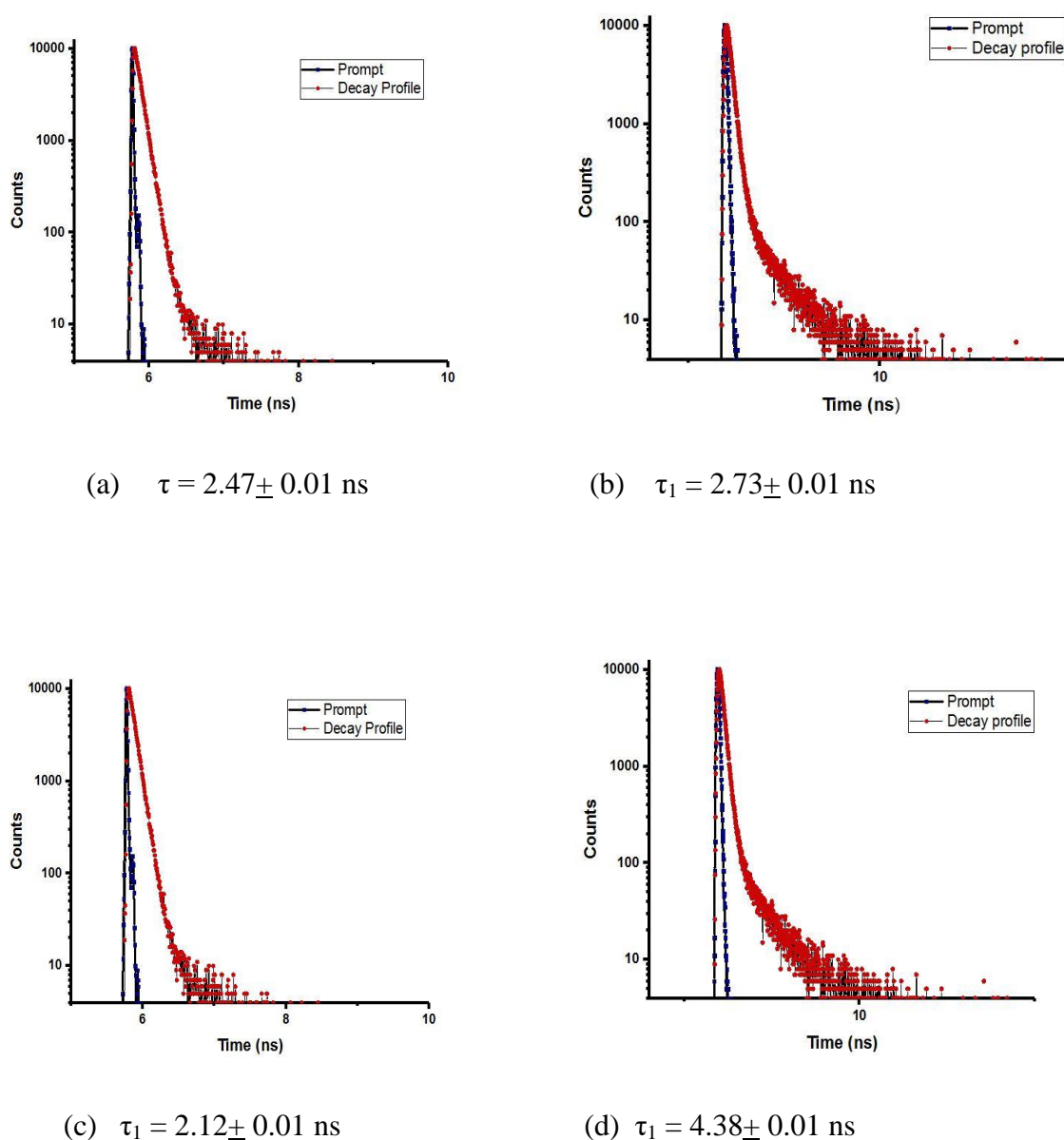


Figure 1.14 Photoluminescence decay of  $10^{-5}$  M solution of C3 in a) THF b) MeCN c) Toluene d) DCM ( $\lambda_{\text{exc}} = 385 \text{ nm}$   $\lambda_{\text{em}} = 450 \text{ nm}$ )



## 1.4 SUMMARY

In this chapter, the electronic properties and potential applications of two different classes of base metal complexes were investigated. A better understanding of the excited state dynamics of these complexes provided an insight in future development of a potential base metal photosensitizer. Probing excited state lifetimes of these complexes and exploring the tenability of the excited state transitions is a first step towards replacing noble metal based photosensitizers.

Heteroleptic metal complexes with donor and acceptor ligands bound to Copper metal were synthesized by an easy and efficient synthetic route. The electronic properties proved to be contradictory to the known literature reports with copper adopting a +1 oxidation state. The excited state dynamics of these complexes were investigated and the influence of donors and acceptors on tuning the MLCT state of these complexes probed thoroughly. Conclusions are strongly supported by TD-DFT calculations defining various transitions. The lifetime of the excited state was estimated in an effort to investigate the potential candidacy of these complexes for photosensitization.

Homoleptic complex with a heavily conjugated ligand bound to an electron rich Zinc metal center was investigated in an effort to understand its electronic properties in detail. The absorption and emission properties of the metal complexes were probed and mechanisms understood. Excited state dynamics and ground state luminescence properties were of special interest in order to assess the potential of the complex for a photosensitization and Light emitting device fabrication.

## Chapter 2

### Investigating Single Electron transfer (SET) mediated Base metal catalysis

---

#### 2.1 INTRODUCTION

Many industrial Catalysts often involve the use of heavy noble metals to drive important chemical reactions. The catalysis cycle generally involves the classic two electron processes - oxidative addition and reductive elimination that involves the change in the oxidation state of metal accompanied by bond dissociation and formation<sup>12</sup>. Recently, there have been numerous reports of base-metal catalysts to drive industrially significant reactions and other chemically difficult reactions<sup>13,14</sup>. This has proved to an effective substitute for the expensive rare metal catalysts<sup>15</sup>. An alternate elegant mechanism to drive catalysis called the single electron transfer has been in use of late. This includes the transfer of an electron to the substrate from an electron rich center to result in the generation of a radical intermediate<sup>16</sup>. The electron rich centers are typically nucleophiles which donate the electron.

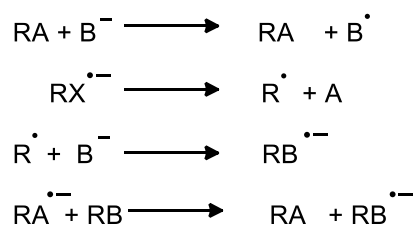


Figure 2.1 S<sub>RN</sub>1 Mechanistic pathway defining SET<sup>17</sup>

Certain redox active ligands have been identified as potential electron reservoirs.<sup>17</sup> They are known to store electron and transfer at a later stage for driving reactions by Single electron transfer.<sup>18</sup> The base metal complexes of such ligands have been established as efficient catalysts with the metal oxidation state not getting disturbed. One such system reported recently is the Hydrosilylation reaction driven by Phenylalanyl ligand bound to Nickel.<sup>19</sup> The Silyl radical generation by Single Electron Transfer assisted by the Nickel Ply catalyst was used to attempt site selective Silylation. The BIAN backbone used as an acceptor earlier is also known to exhibit excellent redox-non innocence behavior. The ability of the backbone to store electrons has also been well established.<sup>20</sup> The Nickel

complex of BIAN has been used to catalyse hydrosilylation of carbonyls and imines mediated by SET. Additionally, Copper(I) systems are well established to catalyse nitrene transfer.<sup>21</sup> Hence, Cu (I) BIANI has been used to establish Nitrene transfer chemistry with BIAN acting as an ancillary support to the Copper(I) metal center.

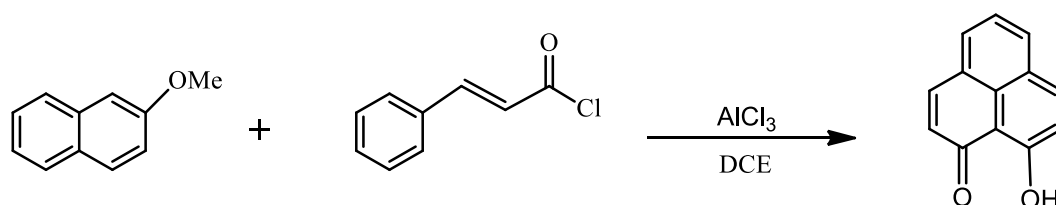
## 2.2 EXPERIMENTAL SECTION

### 2.2.1 Chemicals

Specifications same as mentioned in section 1.2.1

### 2.2.2 Synthesis

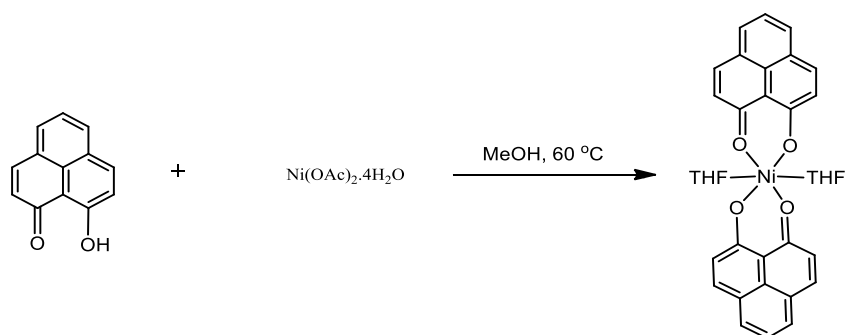
#### 2.2.2.1 Procedure for the Synthesis of Phenylalanine Ligand (PLY)



Scheme 2.1 Synthesis of ligand PLY<sup>19</sup>

2-methoxy naphthalene ( 2 g , 12.6 mM ) and cinnamoyl chloride ( 2.099 g , 12.6 mM ) were added to dichloro ethane (150ml ) taken in a 500ml dry round bottom flask. The Reaction mixture was stirred at 0 °C for half an hour. Anhydrous AlCl<sub>3</sub> (3.36 g, 25.2 mM) was added portion wise ( 1.68 g ) slowly to the reaction mixture for 1 hour and cooled to room temperature. Another portion of AlCl<sub>3</sub> was added slowly and the mixture refluxed at 100°C for 3 hours. The resulting dry cake was cooled and ice was added to facilitate precipitation. Further, dil.HCl was added to neutralize and the precipitate was filtered. The yellow coloured solid was boiled with DCM and filtered through Buchner funnel. The filtrate was extracted in DCM-Water mixture and the organic layer separated. Solvent was removed by rotary-evaporation under reduced pressure and the product separated as a bright yellow solid. The product was further purified by Column Chromatography using Hexane/Ethyl Acetate 97/3 (v/v).

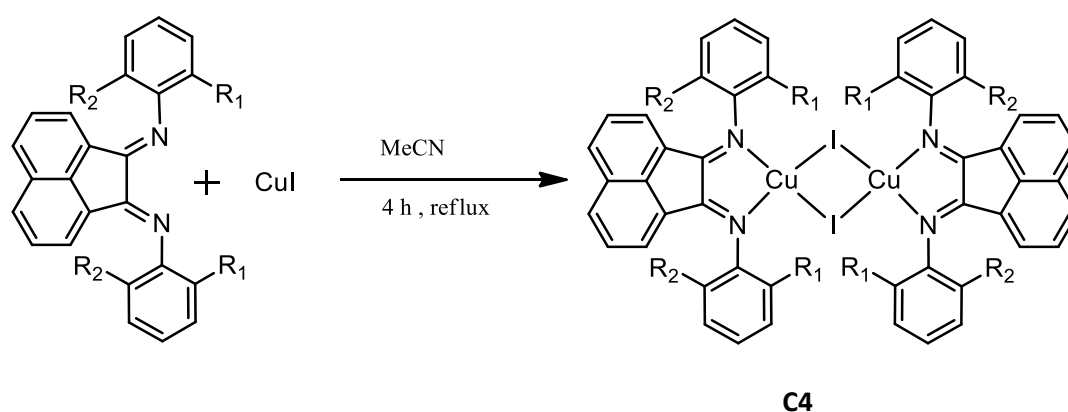
### 2.2.2.2 Procedure for synthesis of Ni(Ply)<sub>2</sub>



Scheme 2.2 Synthesis of the catalyst Ni(Ply)<sub>2</sub><sup>19</sup>

PLY (0.98 g , 5mM ) was dissolved in Methanol ( 50 ml ) in a 100ml dry Round bottom flask and heated to 60°C. In a separate 100ml Round bottom flask, Ni(OAc)<sub>2</sub>·4H<sub>2</sub>O (0.62g , 2.5mM ) was dissolved in 25ml hot Methanol. This solution of Ni(OAc)<sub>2</sub> was added dropwise to the Methanolic solution of PLY and a slow change in the colour from yellow to dark orange was observed. The reaction mixture was further stirred at 60°C for 3 hours and the product precipitated out. The precipitate was filtered and washed with hot Methanol to remove unreacted ligand and metal salt. Crystallization from THF at 5<sup>0</sup>C was attempted.

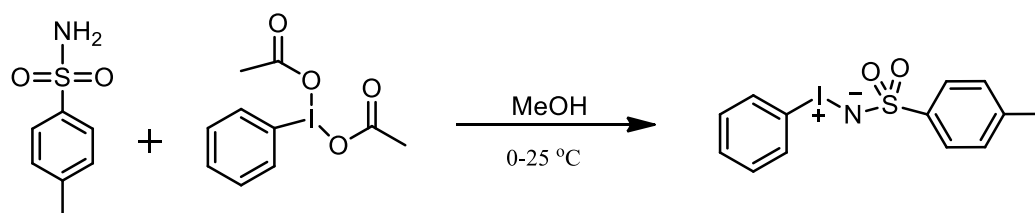
### 2.2.2.3 Procedure for synthesis of ( (BIAN) CuI )<sub>2</sub>



Scheme 2.3 Synthesis of catalyst C4

BIAN ( 200 mg , 15mM ) was added dropwise to a solution of Copper Iodide ( 200 mg , 1mM ) in Acetonitrile ( 25 ml ). The reaction mixture was taken in a dry 100 ml Round bottom flask and heated for 4 hours . The resultant Blue Black product was filtered and crystallised in pure Methanol.

#### 2.2.2.4 Procedure for the synthesis of [N-(p-Toluenesulfonyl) imino]phenyliodinane]

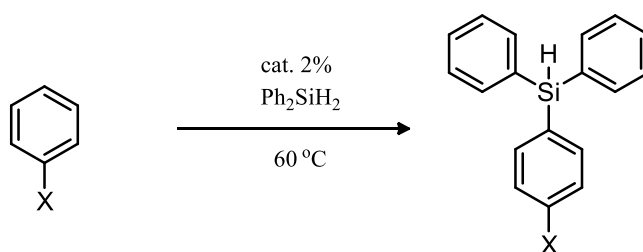


Scheme 2.4 Synthetic procedure of PhInTs<sup>22</sup>

Potassium Hydroxide (2.32 g, 41 mM) was added to p-Toluene sulfonamide (2.8g, 16.4 mM) in Methanol. The reaction mixture was stirred at -10°C for 15 minutes. To this solution,  $\text{PhI}(\text{OAc})_2$  ( 5.3 g , 16.5 mM ) was added slowly and the reaction mixture was further stirred at -10°C for 30 minutes and then at room temperature for additional 3hours. Ice cold water was added to the reaction mixture and precipitation resulted. The white precipitate was filtered and washed with cold methanol. The product was then dried and characterized by  $^1\text{H}$  and  $^{13}\text{C}$  NMR spectroscopies before further catalysis.

#### 2.2.3 Catalysis

##### 2.2.3.1 Site-Selective Silylation

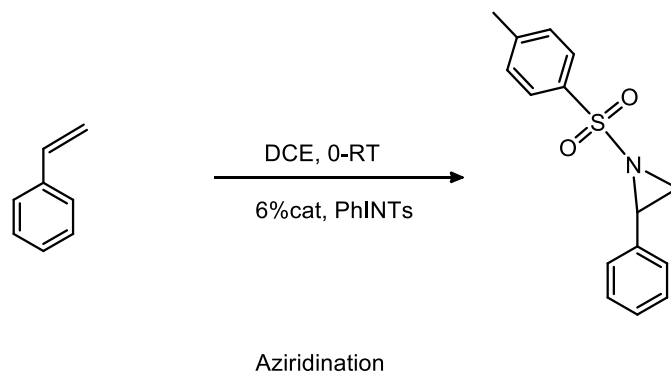


Scheme 2.5 Reaction scheme of silylation

In an overnight oven dried Schlenk flask,  $\text{Ni}(\text{Ply})$  was treated with 2 equivalents of Potassium in dry THF ( 5 ml ). The reaction mixture was stirred overnight at room temperature. After a green colour was observed, the reaction was stopped and the solvent removed under vacuum. The excess Potassium was removed in the glove box and  $\text{Ph}_2\text{SiH}_2$  ( 0.9 ml , 1mM ) was added In Nitrogen atmosphere , 1 equivalent of the substrate was added in 5 ml of dry THF solution and the system was properly packed in a airtight fashion . The reaction mixture was then stirred at 60°C overnight. The solution was concentrated under vacuum and the residue was subjected to column chromatography

with hexane / Ethyl Acetate as eluents. The products were characterized by  $^1\text{H}$  NMR and  $^{13}\text{C}$  NMR spectroscopy.

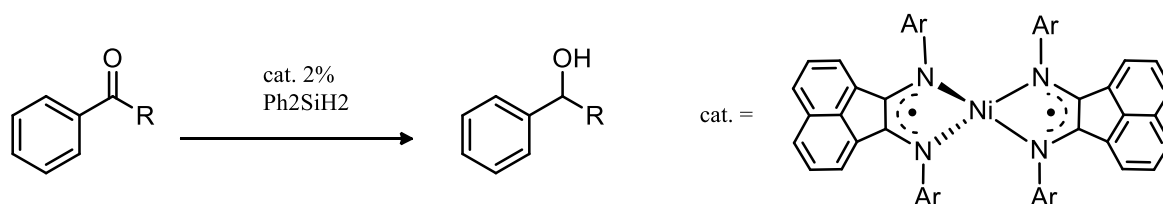
### 2.2.3.2 Aziridination by Nitrene transfer



Scheme 2.6 Reaction scheme for Aziridination

Cu(BIAN)I ( 0.14 mM , 10 mg ) and PhINTs ( 0.24 mM , 89.52 mg ) were added together to an ice cold solution of DCE in a dry schlenk flask . After 5 minutes, under  $\text{N}_2$  atmosphere the substrate was added and the reaction mixture was stirred at  $0^\circ\text{C}$  and gradually taken to room temperature. The stirring continued for 6 to 8 hours and the reaction progress was monitored by TLC. The products were purified by column chromatography with Hexane/Ethyl Acetate 95/5 (v/v).

### 2.2.3.3 SET mediated Hydrosilylation



Scheme 2.7 Reaction scheme for hydrosilylation

In a dry Schlenk flask L1 ( 10 mg , 2mM ) and  $\text{NiCl}_2\cdot\text{DME}$  ( 2 mg , 1 mM ) were added to dry THF ( 5 ml ) . The reaction mixture was treated with 2 equivalents of Potassium and the reaction mixture was stirred overnight at room temperature. In a separate oven dried Schlenk flask,  $\text{Ph}_2\text{SiH}_2$  ( 0.3 ml , 1 eq ) and substrate ( 1 eq. ) were taken and the reduced  $\text{Ni}(\text{BIAN})_2$  solution transferred under Argon atmosphere. The reaction vessel was tightly sealed under Argon and the reaction mixture was stirred for 6 hours at  $60^\circ\text{C}$ . The solution

was concentrated under vacuum and the residue was treated with NaOH and a few drops of water and Methanol. After 3 hours, DCM was added and the product was extracted from the organic layer. The products were further purified by column chromatography using Hexane/Ethyl Acetate 50/50 (v/v). All the products were characterized by  $^1\text{H}$  NMR spectroscopy.

## 2.3 RESULTS AND DISCUSSION

### 2.3.1 Site selective Silylation.

The PLY ligand as a redox storage motif to store and transfer electron for the efficient hydrosilylation reaction of olefins has been reported by Vijayakumar *et al.* recently. Using the same PLY Nickel (II) complex, site selective Silylation of para-substituted phenyl moieties was attempted. The process was envisaged on the ability of the PLY ligand to serve as an electron reservoir and hence could be sequentially reduced to store electrons and transfer at a later stage to generate specific radicals ( Figure 7 ). The hypothesis included the Silyl radical formation by single electron transfer and subsequent C-H bond activation to enable site selective silylation. The general procedure for the catalysis is as described in the experimental section ( 2.2.3.1 ).

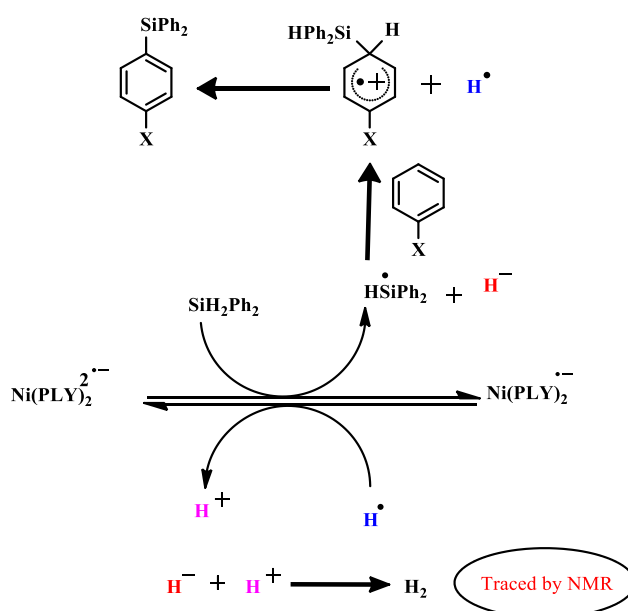


Figure 2.2 Hypothesis of site selective C-H activation mediated by SET

### 2.3.1.1 Reaction Optimization

The reaction conditions were varied and the progress of the reaction monitored by Thin layer Chromatography. The optimization conditions included varying the reaction temperatures and duration of the reaction. Upon completion of 6 hours, the extra spot apart from the reactants was visualized in the Thin layer chromatography indicating the formation of product.

| S.No | Temperature (°C) | Time ( hours) | Result             |
|------|------------------|---------------|--------------------|
| 1    | 40               | 6             | Reactants remained |
| 2    | 50               | 6             | Reactants remained |
| 3    | 60               | 6             | Product Formation  |

Table 2.1 Optimization conditions for the reaction by varying reaction temperature

The product was isolated by column chromatography using hexane/ethyl acetate 95/5 (v/v) and characterized by  $^1\text{H}$  and  $^{13}\text{C}$  NMR spectroscopy and the results analyzed.

### 2.3.1.2 Silylation results

The reaction upon monitoring by  $^1\text{H}$  NMR showed a continuous consumption of Diphenylsilane with time indicating forward progress of the reaction in substrates with halogen substitution in the 4' position. However, contrary to the originally conceived hypothesis, the generated Silyl radical mediated by the single electron transfer from the PLY backbone happened to activate the highly activated C-X bond in the Halogen substituted substrates. This resulted in the formation of Triphenylsilane as characterized by  $^1\text{H}$  NMR leading to Dehalosilylation. The reaction was not successful in substrates with other substitutions.



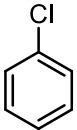
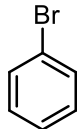
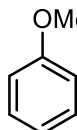
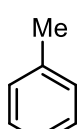
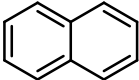
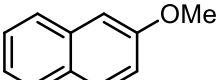
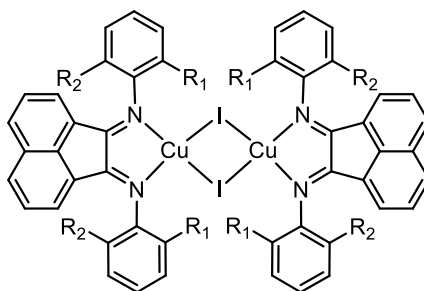
| S.No | SUBSTRATE   | % YIELD        |
|------|---|----------------|
| 1    |    | C-X activation |
| 2    |    | C-X activation |
| 3    |    | No reaction    |
| 4    |    | No reaction    |
| 5    |   | No reaction    |
| 6    |  | No reaction    |

Table 2.2 Summary of Results and Analysis

## 2.3.2 Aziridination by Nitrene transfer

### 2.3.2.1 The Catalyst

The catalyst Cu(BIAN)I **C4** was characterized by various analytical tools like X-Ray Diffraction of the crystal structure (Fig 8), high resolution mass spectrometry (Fig.9) as a means of assessing its nature in solution and solid state. The electronic properties of the catalyst in the ground state were understood by means of UV-Vis spectroscopy (Fig.10)



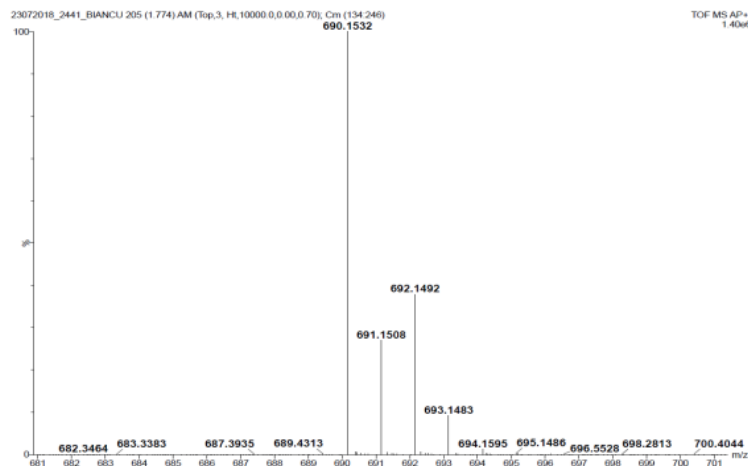


Figure 2.3 The HRMS spectrum of **C4** indicates the monomeric nature in solution.

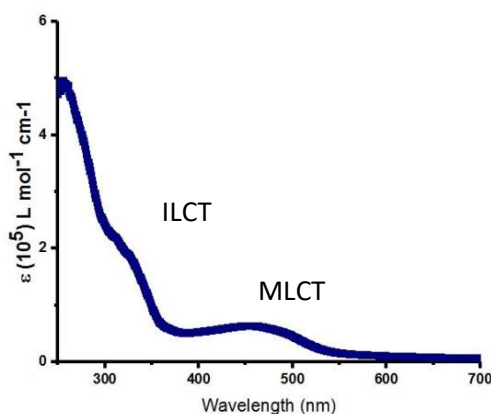


Figure 2.4 UV-Vis absorption spectrum of  $10^{-5}$  M solution of **C4** in DCM at RT.

### 2.3.2.2 Substrate Scope

Aziridine – a commercially important three membered heterocycle formation from alkenes using an economically viable and efficient catalyst (**C4**) has been established with a good yield and is established to be a fairly general reaction.

The reaction is established to be successful for a wide variety of aromatic olefins irrespective of the presence of electron donating or electron withdrawing substituents as well as aliphatic alkenes. Aziridination catalyzed by **C4** is successful while using a wide variety of Nitrene sources (Chloramine T, PhINTs and Azides). Optimization of Reaction conditions w using Chloramine T and Azides as Nitrene sources is currently underway.

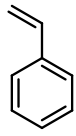
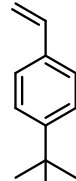
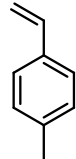
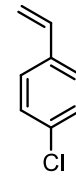
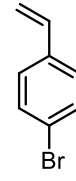
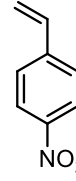
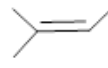
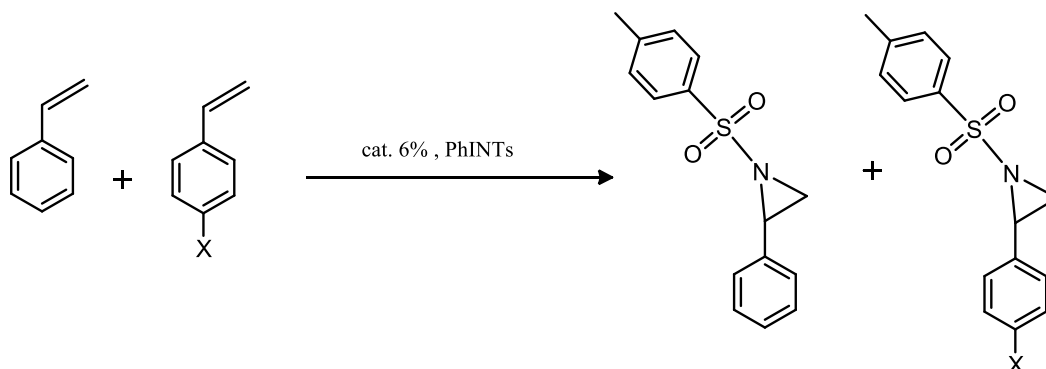
| S.No | SUBSTRATE   | % YIELD |
|------|---|---------|
| 1    |    | 60%     |
| 2    |    | 85%     |
| 3    |    | 93%     |
| 4    |   | 78%     |
| 5    |  | 79%     |
| 6    |  | 13.12%  |
| 7    |  | 85%     |

Table 2.3 Summary of substrate scope establishing generality of the reaction.

### 2.3.2.3 The Hammett Correlation

Competitive experiments were performed with both styrene and substituted styrene as substrates. The percentage of conversion of substituted Styrene to Aziridine with respect to the unsubstituted styrene conversion was estimated and quantified by NMR with Ferrocene as internal standard. The Logarithm of yields vs. the Dual parameter fitting

coefficient (Linear combination of coefficients representing the polar and radical effects of the substituents on the alkene carbon) is called the Hammett correlation (Figure9).



Scheme 2.8 Competitive experiments to establish Hammett correlation

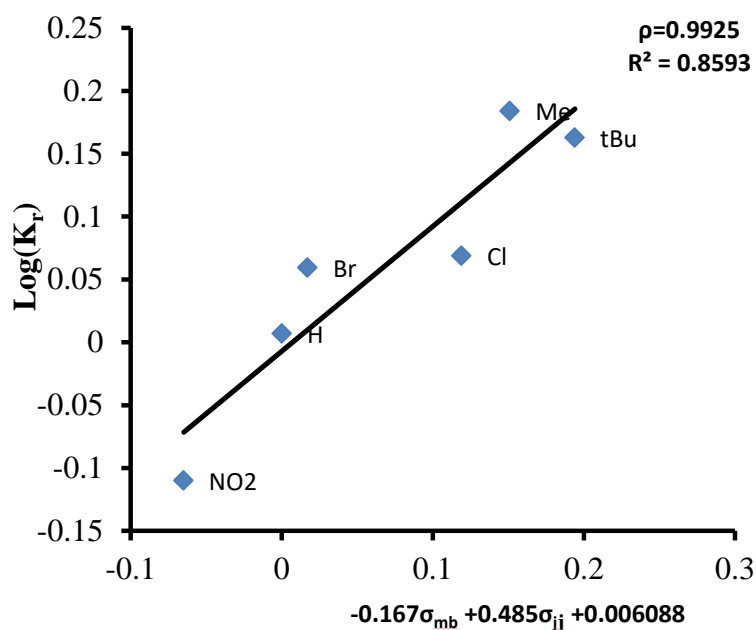


Figure 2.5 Dual parameter Hammett fit indicating the dominant radical effect.

A positive slope of the Hammett plot indicates the substituent effects are mostly radical in nature. This intriguing result is currently under investigation to conclusively establish the reaction mechanism.

## 2.3.3 Nickel assisted catalytic Hydrosilylation

### 2.3.3.1 Proposed hypothesis

An industrially significant reaction, Hydrosilylation of aldehydes and ketones were attempted by SET mediated catalysis as opposed to the conventional catalysis involving oxidative addition and reductive elimination. The catalyst is one electron reduced Nickel (II) chelated to **L1** on both sides. The ability of **L1** to store electron and transfer it at a later stage is effectively utilized to drive the reaction. The mechanism proposed is elaborated in Figure 10. Sequential one electron reduction of the catalyst is followed by addition of Diphenylsilane and the substrate. The detailed experimental procedure for catalysis is as described in the experimental section.

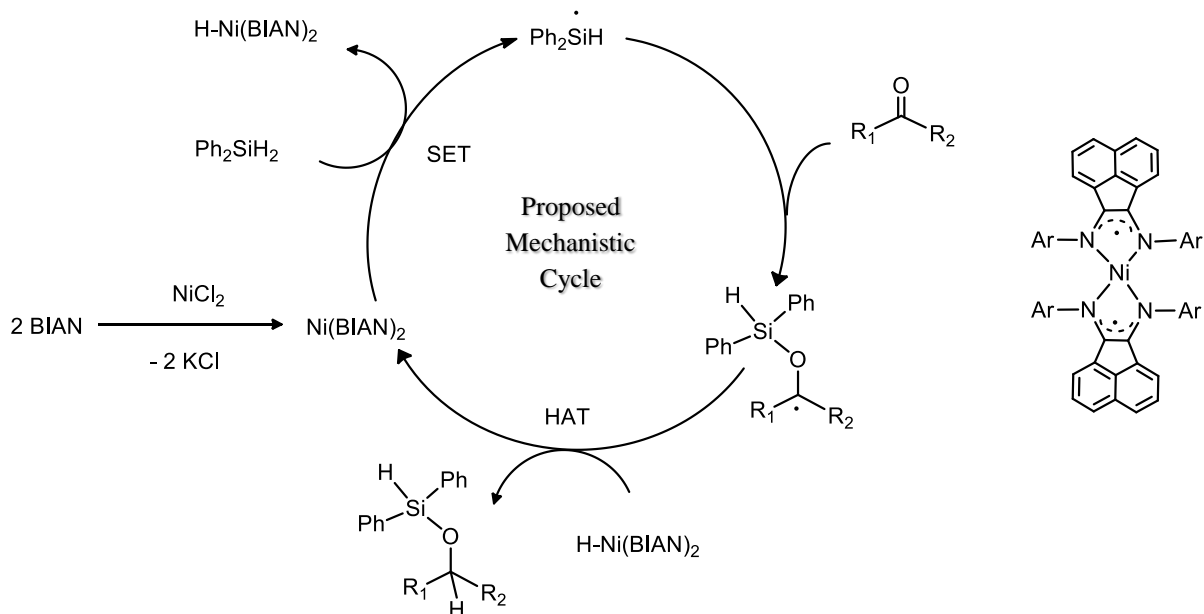
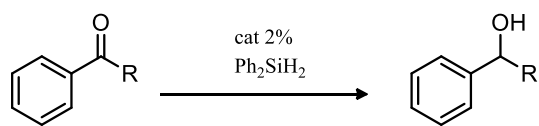


Figure 2.6 Proposed mechanism for SET mediated Hydrosilylation

### 2.3.3.2 Substrate Scope

The reaction is found to be successfully catalyzed for a wide variety of substrates including Aldehydes, Ketones and imines. Substantial yield is also obtained for both aromatic and aliphatic aldehydes and ketones. The success of the catalysis for such a diverse spectrum of the substrates (Table 6) establishes the general nature of the catalyst. The excellent efficiency of the catalyst is substantiated by the good yields at 2% catalyst loading.



| S.No | SUBSTRATE | % YIELD |
|------|-----------|---------|
| 1    |           | 97%     |
| 2    |           | 95%     |
| 3    |           | 98%     |
| 4    |           | 90%     |
| 5    |           | 85%     |
| 6    |           | 87%     |
| 7    |           | 75%     |

Table 2.4 The Diverse substrate scope establishing the generality of the reaction.

## 2.4 Summary

Three different catalysts operating by distinct mechanisms to drive three significant chemical reactions have been explored. The common goal underlying all three mechanisms is to provide an efficient and economically viable base metal alternative to the conventional heavy Noble metal catalysts. The catalyst design principle is to coordinate base metal with redox non innocent ligands on either side as potential electron reservoirs.

The Nickel (II) ply complex upon single electron reduction was tested for the generation of silyl radical by SET to further Silylate in the para position of substituted benzenes by site selective C-H activation. The Silyl radical generation was successful and Silylation progressed by C-X bond activation in case of halobenzene substrates. The reaction was observed to be not successful in other substituted substrates.

Aziridination reaction catalyzed by Cu(I) metal center bound to BIAN which serves as ancillary ligand was proved to be successful. With the efficiency and the general nature of the catalyst were substantiated considerably, a thorough understanding of the nature of the reaction mechanism was obtained by Hammett analysis.

The BIAN ligand bound to a Nickel(II) center was investigated as an efficient catalyst to mediate single electron transfer for catalyzing hydrosilylation reaction. The catalysis was established to be successful and efficient substantiated by good yields with minimal catalyst loading.

## BIBLIOGRAPHY

- (1) Meyer, T. J. Photochemistry of Metal Coordination Complexes: Metal to Ligand Charge Transfer Excited States. *Pure Appl. Chem.* **1986**, 58 (9), 1193–1206.
- (2) Gu, B.; Wu, W.; Xu, G.; Feng, G.; Yin, F.; Chong, P. H. J.; Qu, J.; Yong, K.-T.; Liu, B. Precise Two-Photon Photodynamic Therapy Using an Efficient Photosensitizer with Aggregation-Induced Emission Characteristics. *Adv. Mater.* **2017**, 29 (28), 1701-1706.
- (3) Hara, K.; Sayama, K.; Arakawa, H.; Ohga, Y.; Shinpo, A.; Suga, S. A Coumarin-Derivative Dye Sensitized Nanocrystalline TiO<sub>2</sub> Solar Cell Having a High Solar-Energy Conversion Efficiency up to 5.6%. *Chem. Commun.* **2001**, 0 (6), 569–570.
- (4) Pal, A. K.; Nag, S.; Ferreira, J. G.; Brochery, V.; La Ganga, G.; Santoro, A.; Serroni, S.; Campagna, S.; Hanan, G. S. Red-Emitting [Ru(Bpy)<sub>2</sub>(N-N)]<sup>2+</sup> Photosensitizers: Emission from a Ruthenium(II) to 2,2'-Bipyridine<sup>3</sup> MLCT State in the Presence of Neutral Ancillary “Super Donor” Ligands. *Inorg. Chem.* **2014**, 53 (3), 1679–1689.
- (5) Ferrere, S. New Photosensitizers Based upon [Fe(L)<sub>2</sub>(CN)<sub>2</sub>] and [Fe(L)<sub>3</sub>] (L = Substituted 2,2'-Bipyridine): Yields for the Photosensitization of TiO<sub>2</sub> and Effects on the Band Selectivity. *Chem. Mater.* **2000**, 12 (4), 1083–1089.
- (6) Durham, B.; Caspar, J. V.; Nagle, J. K.; Meyer, T. J. Photochemistry of Tris(2,2'-Bipyridine)Ruthenium(2+) Ion. *J. Am. Chem. Soc.* **1982**, 104 (18), 4803–4810.
- (7) Cameron, L. A.; Ziller, J. W.; Heyduk, A. F. Near-IR Absorbing Donor–Acceptor Ligand-to-Ligand Charge-Transfer Complexes of Nickel(II). *Chem. Sci.* **2016**, 7 (3),
- (8) Chen, L. X.; Shaw, G. B.; Novozhilova, I.; Liu, T.; Jennings, G.; Attenkofer, K.; Meyer, G. J.; Coppens, P. MLCT State Structure and Dynamics of a Copper(I) Diimine Complex Characterized by Pump-Probe x-Ray and Laser Spectroscopies and DFT Calculations. *J. Am. Chem. Soc.* **2003**, 125 (23), 7022–7034.
- (9) Kramer, W. W.; Cameron, L. A.; Zarkesh, R. A.; Ziller, J. W.; Heyduk, A. F. Donor–Acceptor Ligand-to-Ligand Charge-Transfer Coordination Complexes of

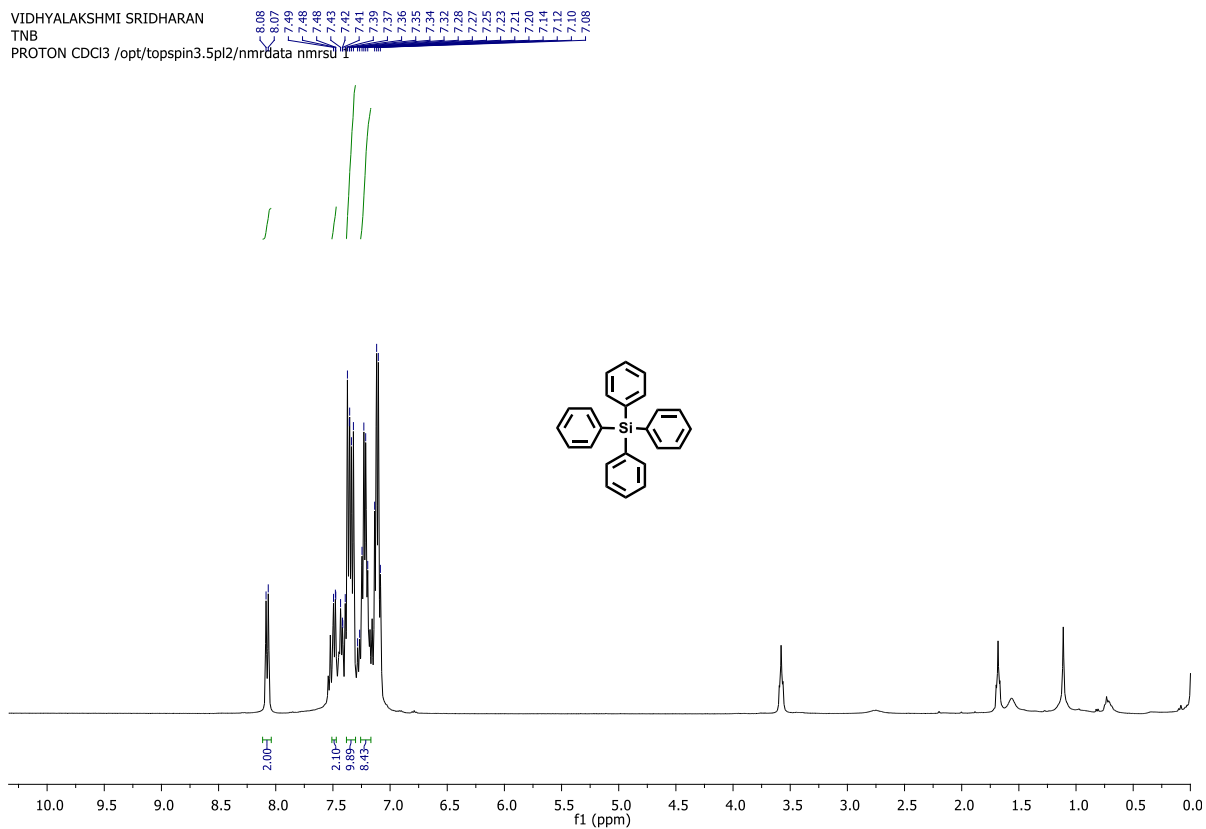


- Nickel(II). *Inorg. Chem.* **2014**, *53* (16), 8825–8837..
- (10) McCusker, C. E.; Castellano, F. N. Design of a Long-Lifetime, Earth-Abundant, Aqueous Compatible Cu(I) Photosensitizer Using Cooperative Steric Effects. *Inorg. Chem.* **2013**, *52* (14), 8114–8120.
- (11) Brown, D. G.; Hughes, W. J.; Knerr, G. Electronic and X-Ray Photoelectron Spectra of Copper Catecholate Complexes. *Inorganica Chim. Acta* **1980**, *46*, 123–126.
- (12) Lu, E.; Liddle, S. T. Uranium-Mediated Oxidative Addition and Reductive Elimination. *Dalt. Trans.* **2015**, *44* (29), 12924–12941.
- (13) Yoshikai, N. Cp\*Co<sup>III</sup>-Catalyzed C–H Activation of (Hetero)Arenes: Expanding the Scope of Base-Metal-Catalyzed C–H Functionalizations. *ChemCatChem* **2015**, *7* (5), 732–734.
- (14) Wright, W. R. H.; Berkeley, E. R.; Alden, L. R.; Baker, R. T.; Sneddon, L. G. Transition Metal Catalysed Ammonia-Borane Dehydrogenation in Ionic Liquids. *Chem. Commun.* **2011**, *47* (11), 3177–3179.
- (15) Carril, M.; SanMartin, R.; Domínguez, E. Palladium and Copper-Catalysed Arylation Reactions in the Presence of Water, with a Focus on Carbon–Heteroatom Bond Formation. *Chem. Soc. Rev.* **2008**, *37* (4), 639–647.
- (16) Ashby, E. C. Single-Electron Transfer, a Major Reaction Pathway in Organic Chemistry. An Answer to Recent Criticisms. *Acc. Chem. Res.* **1988**, *21* (11), 414–421.
- (17) Dzik, W. I.; Van Der Vlugt, J. I.; Reek, J. N. H.; De Bruin, B. Ligands That Store and Release Electrons during Catalysis. *Angew. Chemie - Int. Ed.* **2011**, *50* (15), 3356–3358.
- (18) Pan, Q.; Freitag, L.; Kowacs, T.; Falgenhauer, J. C.; Korterik, J. P.; Schlettwein, D.; Browne, W. R.; Pryce, M. T.; Rau, S.; González, L.; et al. Peripheral Ligands as Electron Storage Reservoirs and Their Role in Enhancement of Photocatalytic Hydrogen Generation. *Chem. Commun.* **2016**, *52* (60), 9371–9374.
- (19) Vijaykumar, G.; Pariyar, A.; Ahmed, J.; Shaw, B. K.; Adhikari, D.; Mandal, S. K.

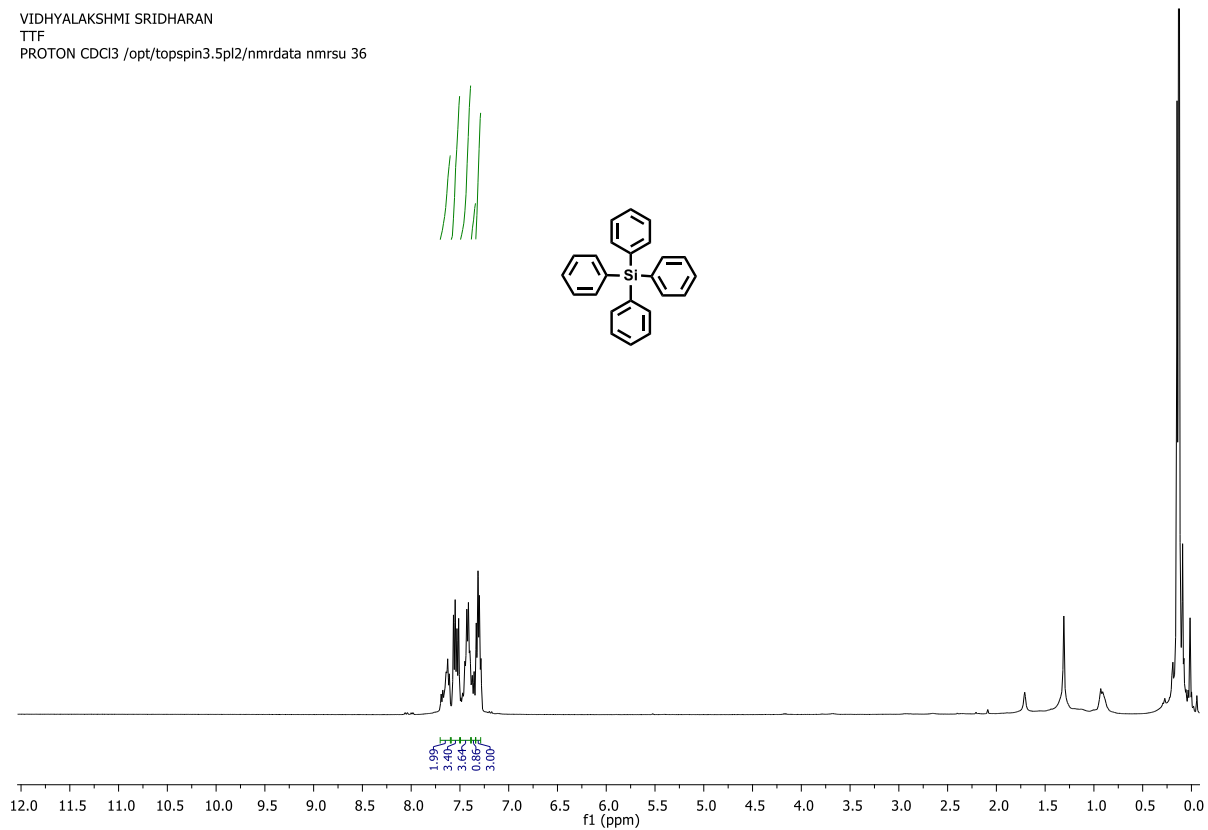
- Tuning the Redox Non-Innocence of a Phenalenyl Ligand toward Efficient Nickel-Assisted Catalytic Hydrosilylation. *Chem. Sci.* **2018**, *9* (10), 2817–2825.
- (20) Singha Hazari, A.; Ray, R.; Hoque, M. A.; Lahiri, G. K. Electronic Structure and Multicatalytic Features of Redox-Active Bis(Arylimino)Acenaphthene (BIAN)-Derived Ruthenium Complexes. *Inorg. Chem.* **2016**, *55* (16), 8160–8173.
- (21) Peter Brandt, †,§; Mikael J. Södergren, ‡; Pher G. Andersson, \*,‡ and; Per-Ola Norrby\*, †. Mechanistic Studies of Copper-Catalyzed Alkene Aziridination. **2000**.
- (22) Maestre, L.; Frutos, M. R.; Díaz-Requejo, M. M.; Pérez, P. J. Copper-Catalyzed Nitrene Transfer as a Tool for the Synthesis of N-Substituted 1,2-Dihydro- and 1,2,3,4-Tetrahydropyridines. *Organometallics* **2012**, *31* (22), 7839–7843.

# APPENDIX

VIDHYALAKSHMI SRIDHARAN  
TNB  
PROTON CDCl3 /opt/topspin3.5pl2/nmrdata nmrsu 1

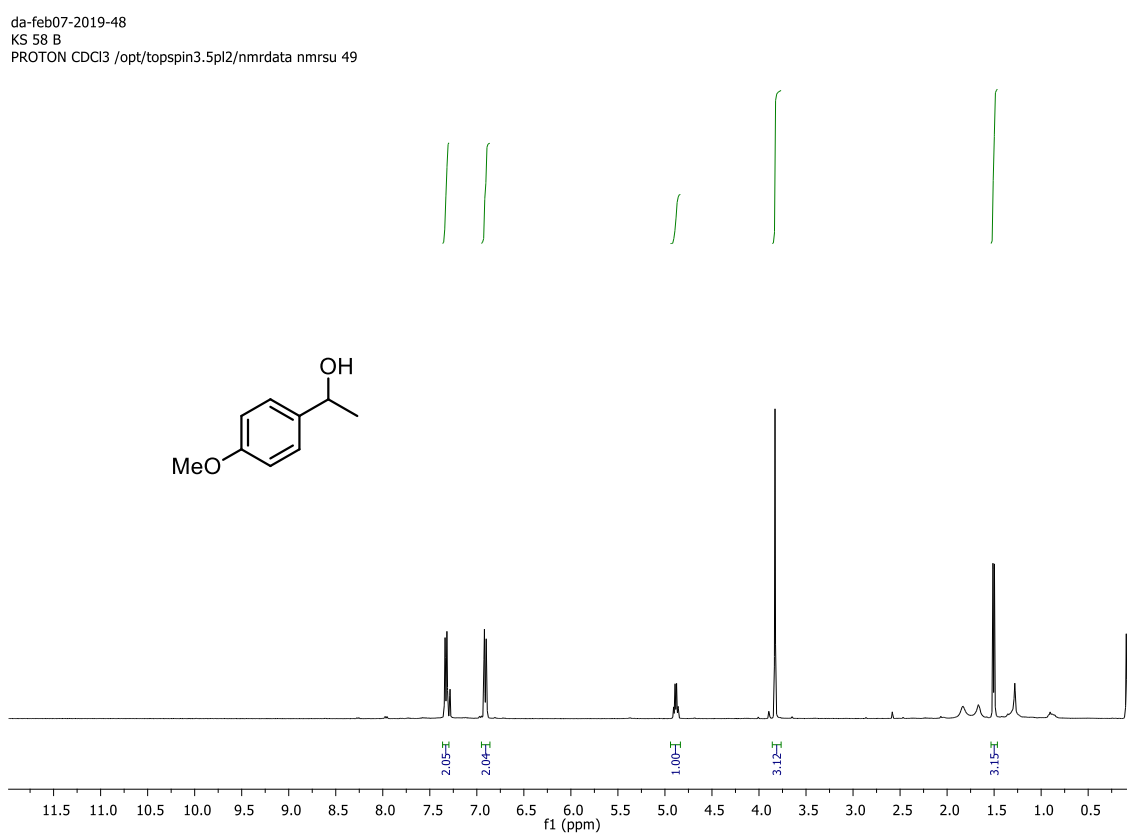


VIDHYALAKSHMI SRIDHARAN  
TTF  
PROTON CDCl3 /opt/topspin3.5pl2/nmrdata nmrsu 36

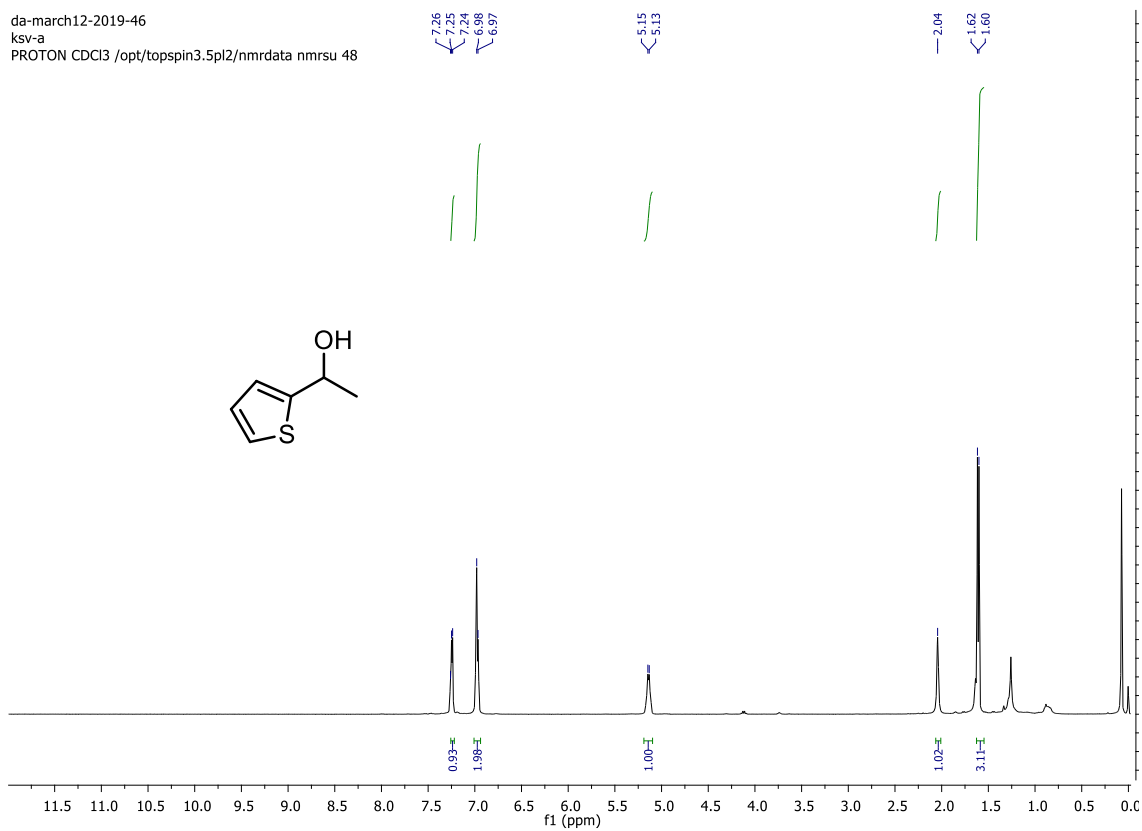


# APPENDIX

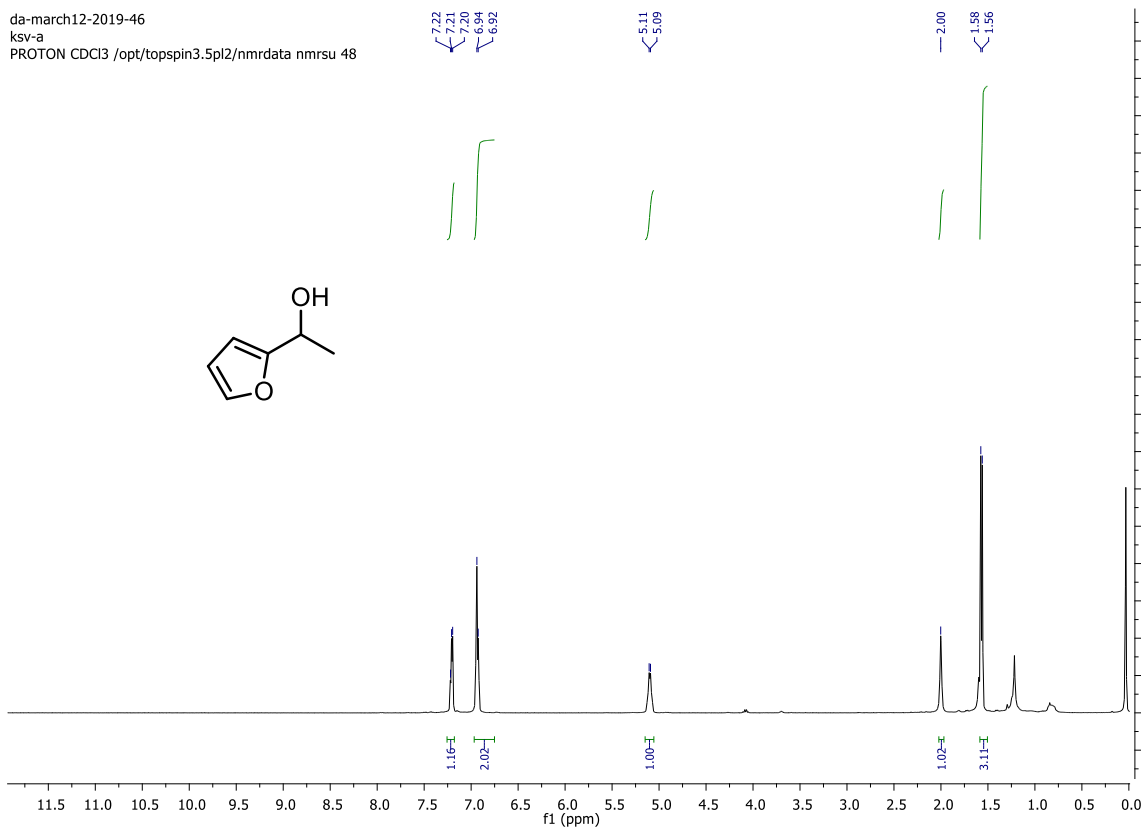
da-feb07-2019-48  
KS 58 B  
PROTON CDCl3 /opt/topspin3.5pl2/nmrdata nmsu 49



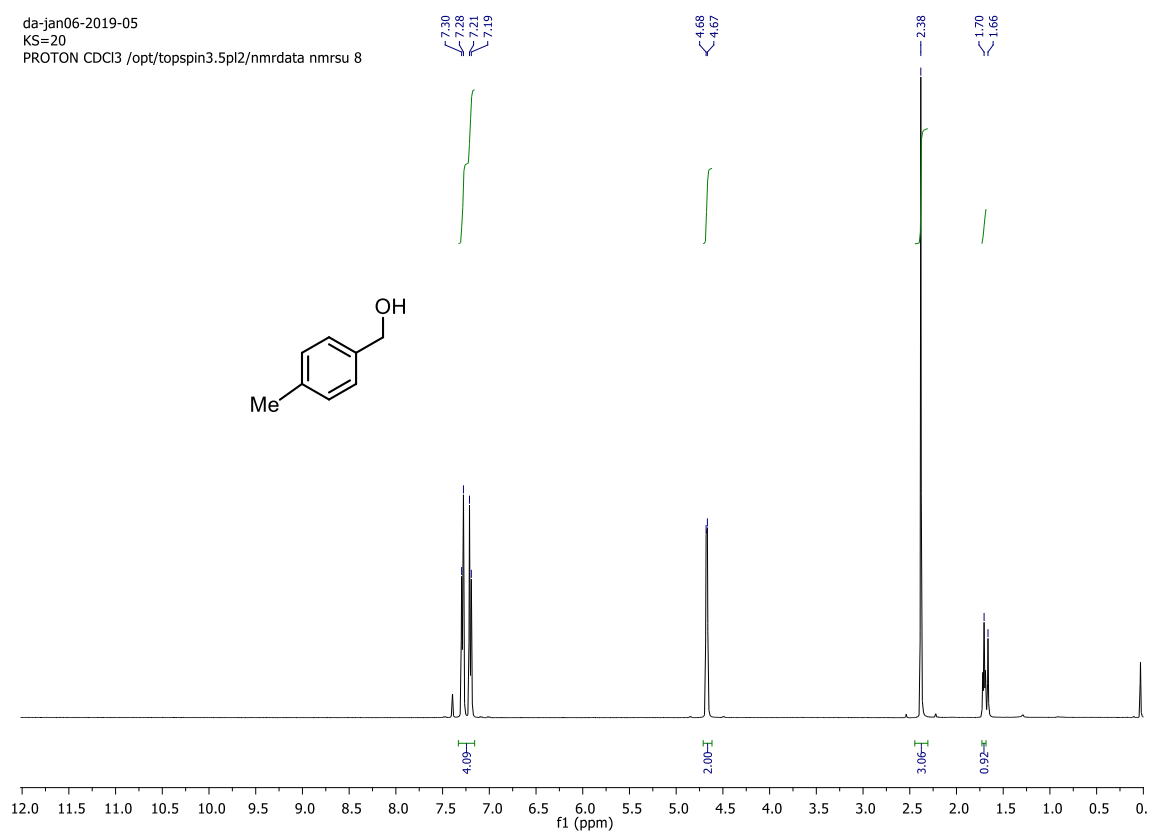
da-march12-2019-46  
ksv-a  
PROTON CDCl3 /opt/topspin3.5pl2/nmrdata nmsu 48



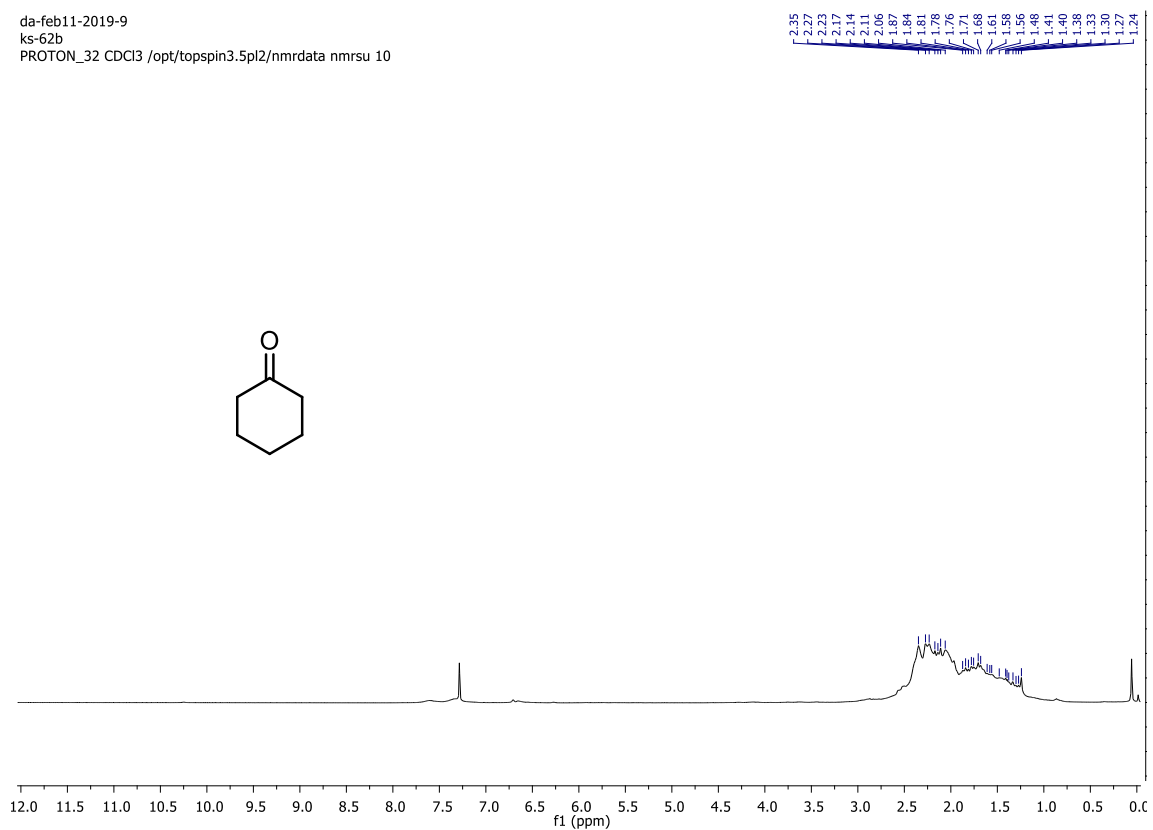
da-march12-2019-46  
ksv-a  
PROTON CDCl3 /opt/topspin3.5pl2/nmrdata nmrsu 48



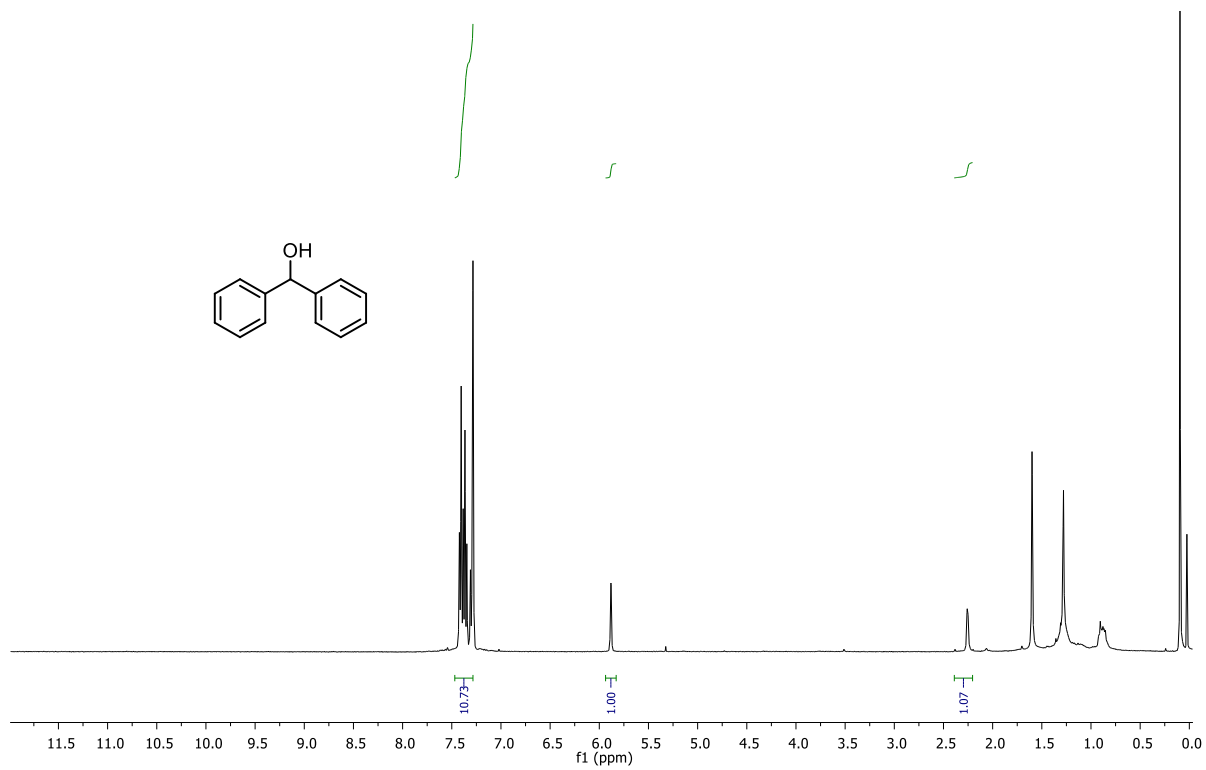
da-jan06-2019-05  
KS=20  
PROTON CDCl3 /opt/topspin3.5pl2/nmrdata nmrsu 8



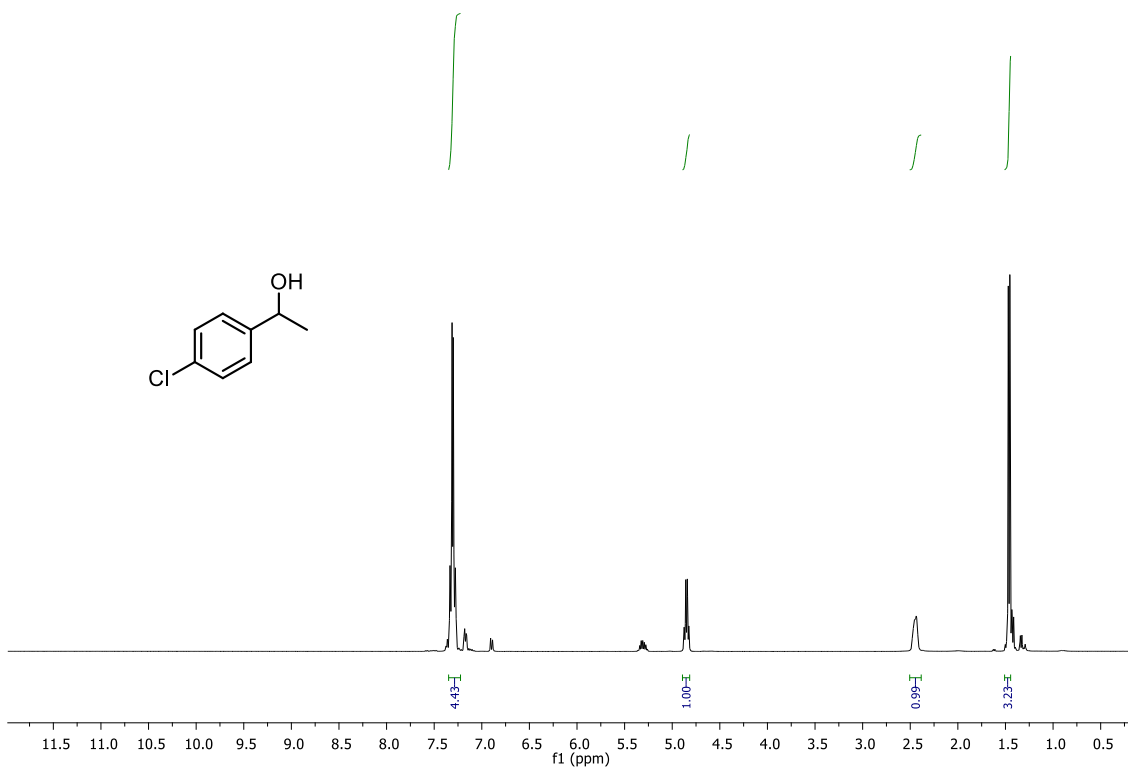
da-feb11-2019-9  
ks-62b  
PROTON\_32 CDCl3 /opt/topspin3.5pl2/nmrdata nmrsu 10



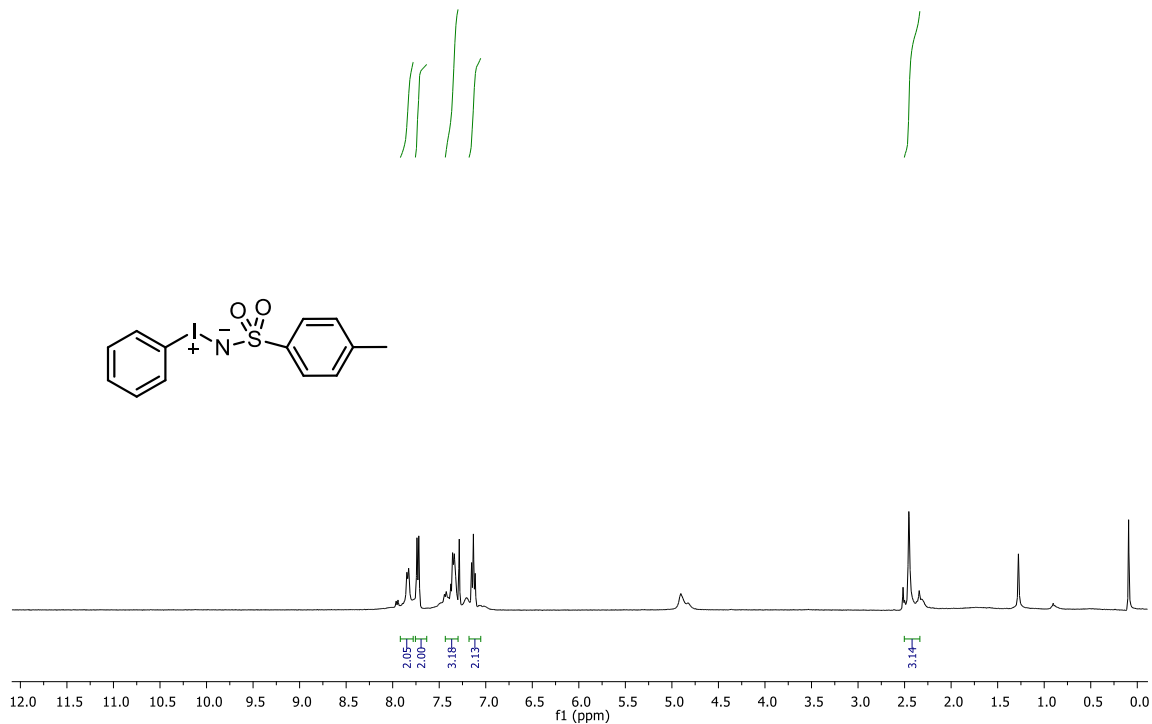
da-feb20-2019-22  
KSV 55 B  
PROTON CDCl3 /opt/topspin3.5pl2/nmrdata nmrsu 24



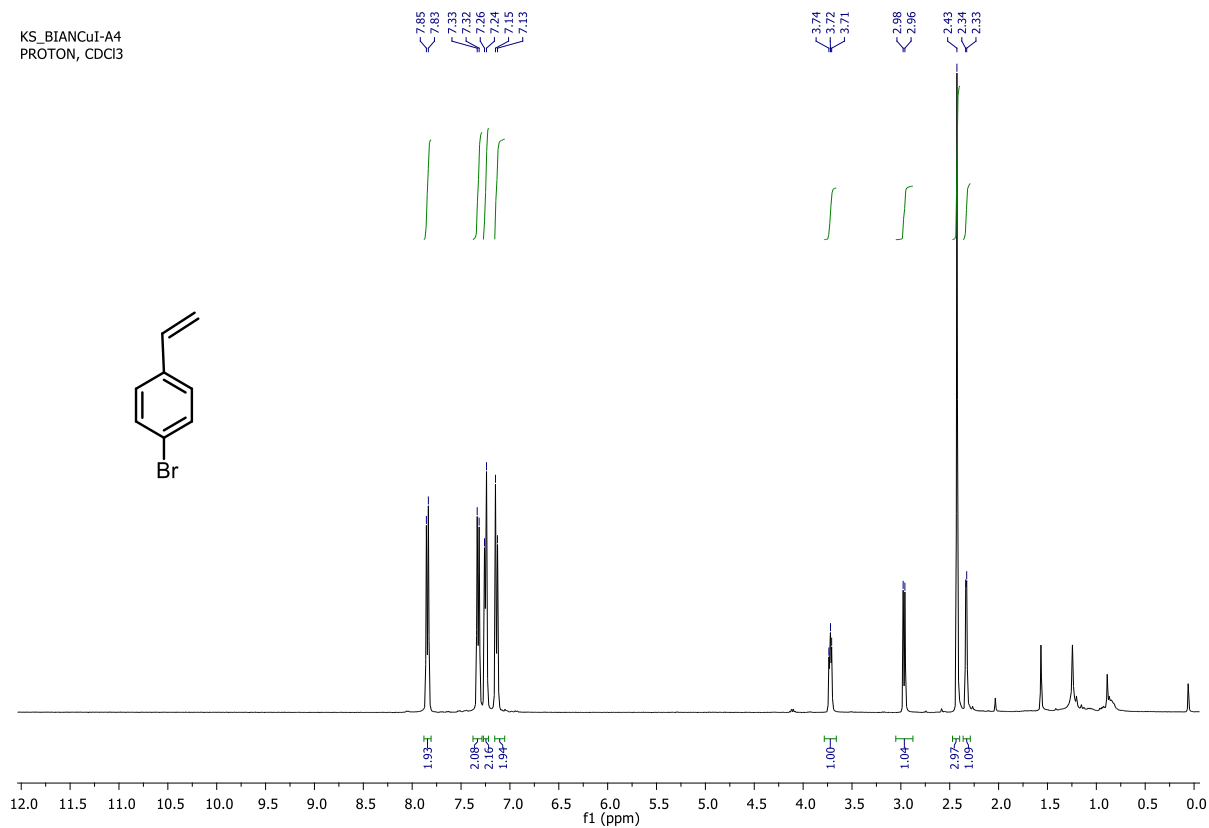
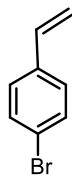
da-march12-2019-46  
ksv-d  
PROTON CDCl3 /opt/topspin3.5pl2/nmrdata nmrsu 47



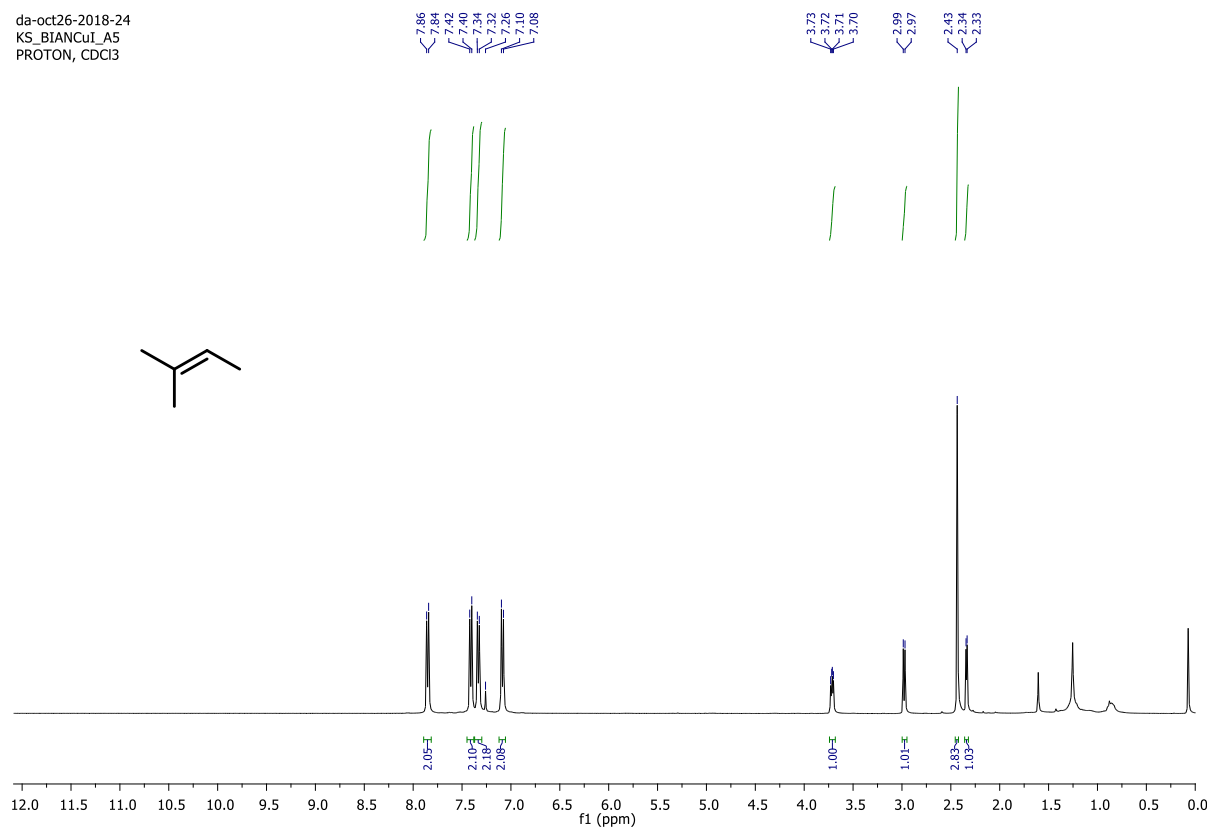
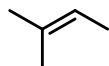
da-oct24-2018-23  
KS PHI NT3  
PROTON CDCl3 /opt/topspin3.5pl2/nmrdata nmrsu 28



KS\_BIANCuI-A4  
PROTON, CDCl3

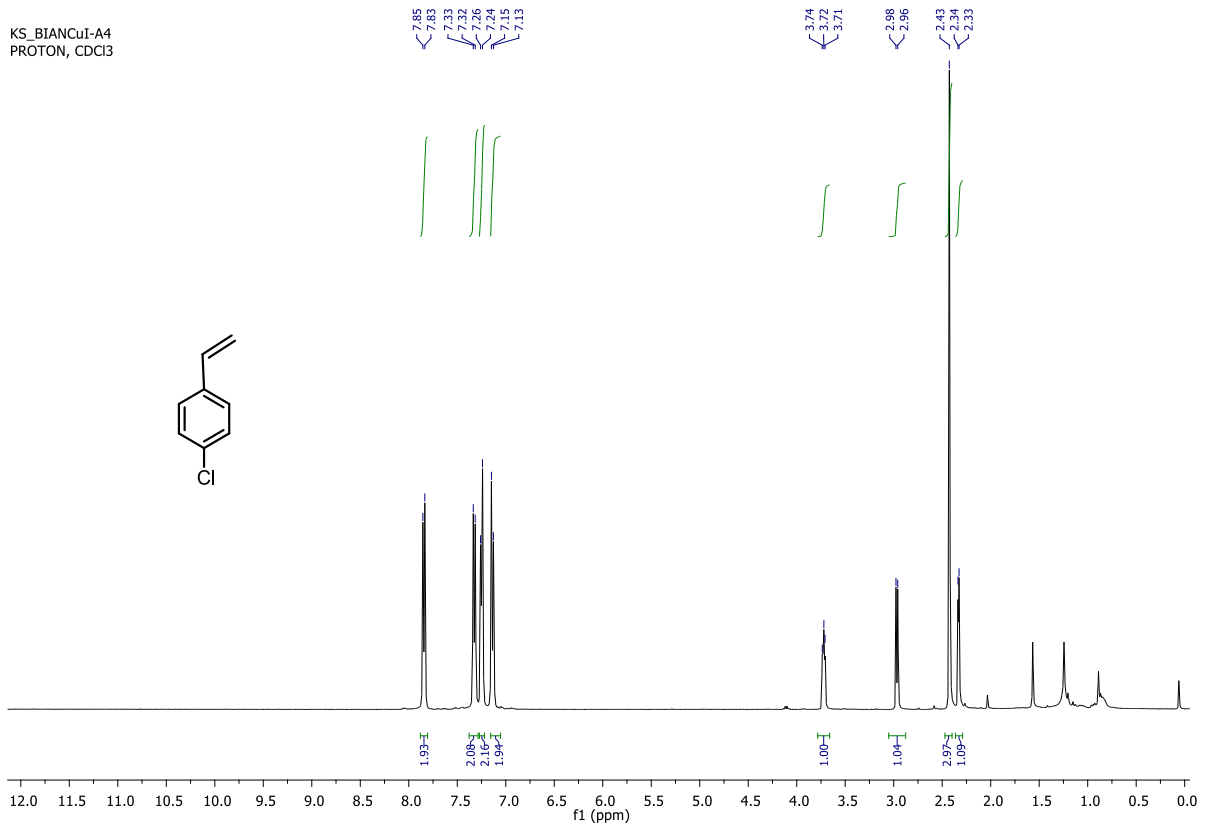


da-oct26-2018-24  
KS\_BIANCuI\_A5  
PROTON, CDCl3

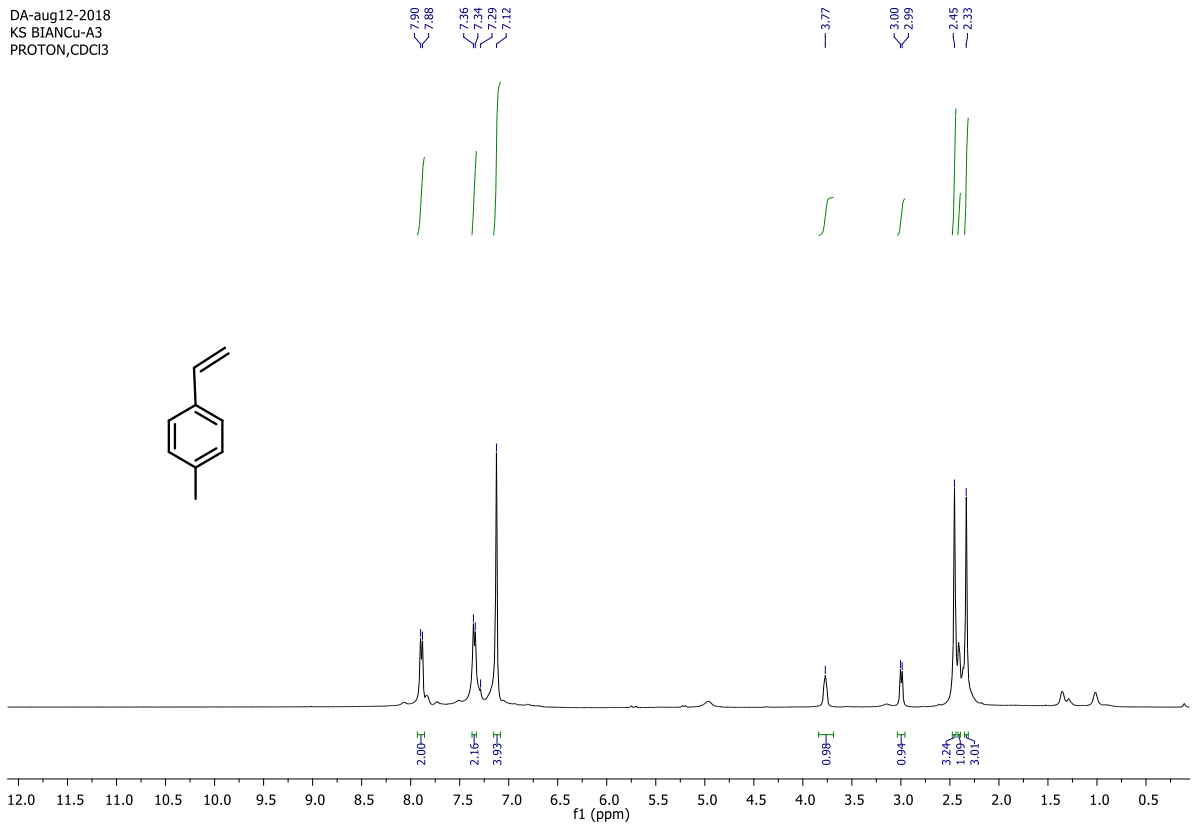




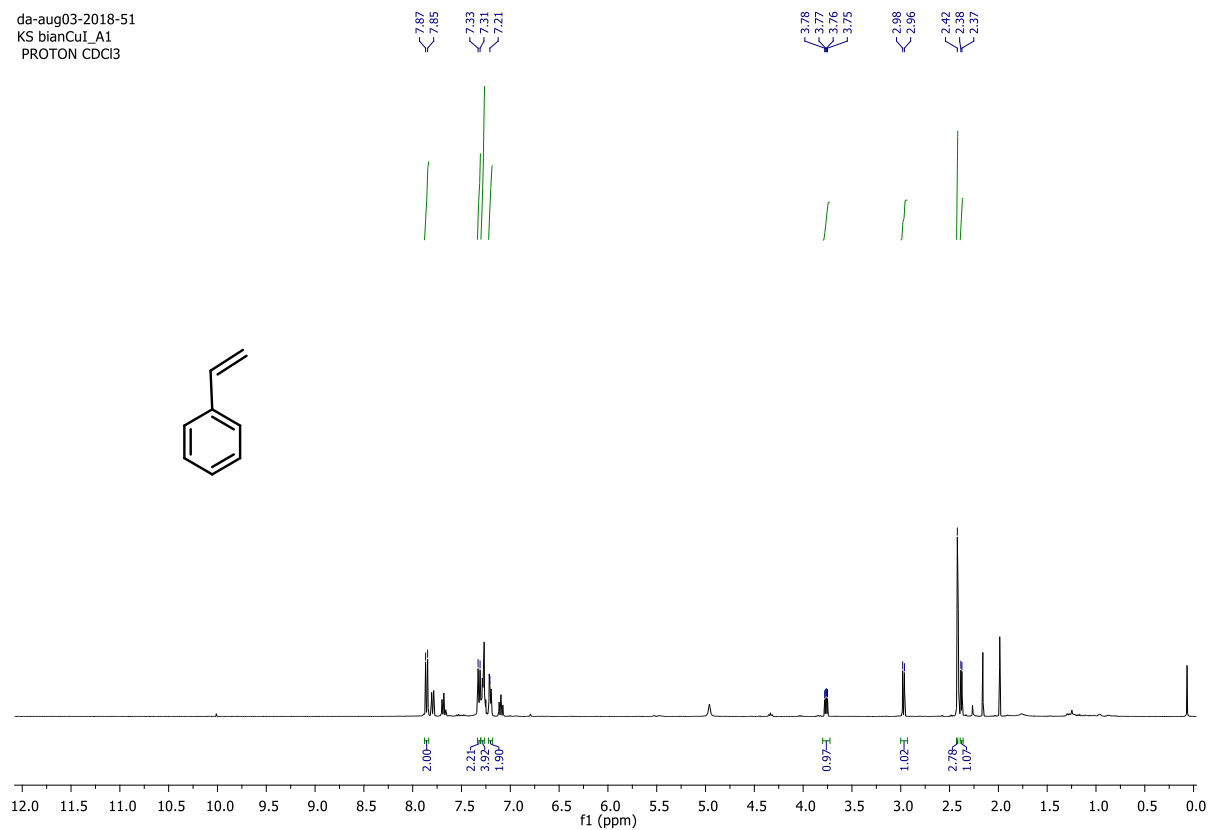
KS\_BIANCu1-A4  
PROTON, CDCl3



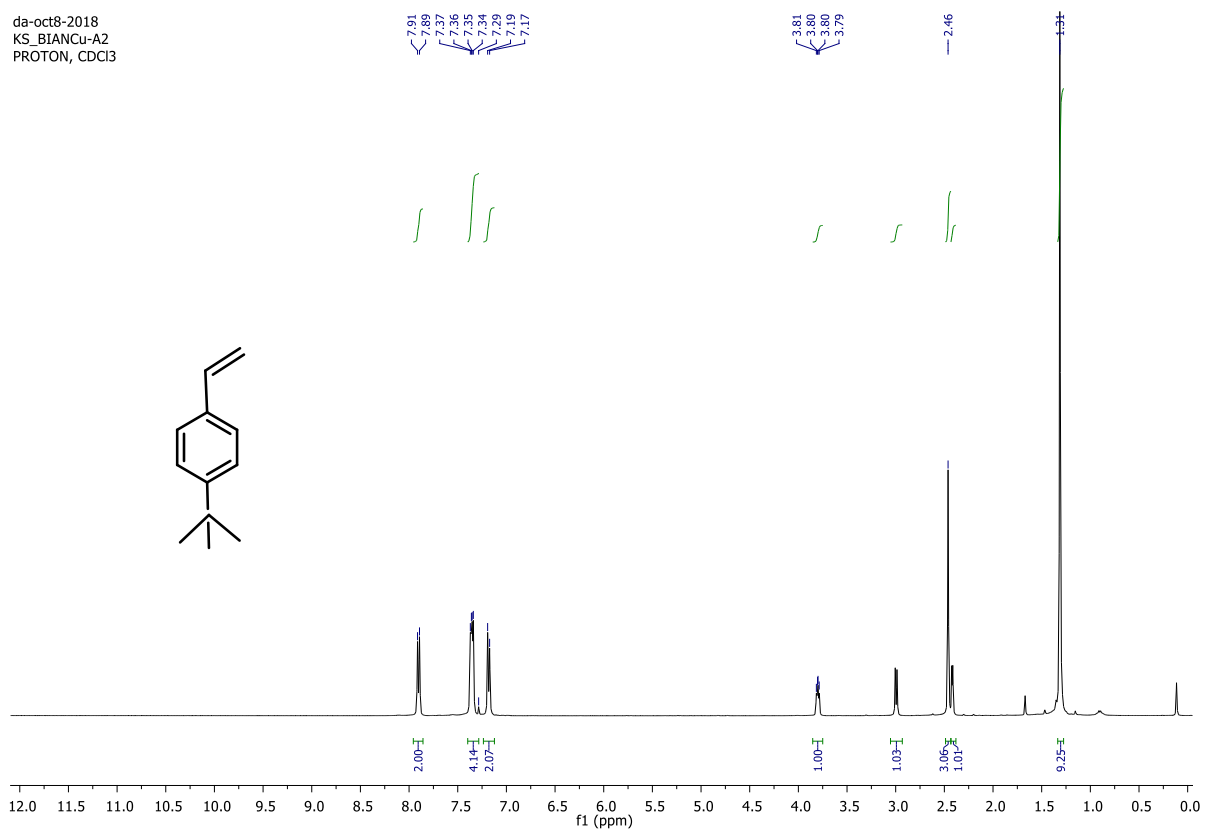
DA-aug12-2018  
KS\_BIANCu-A3  
PROTON, CDCl3



da-aug03-2018-51  
KS bianCu\_A1  
PROTON CDCl3



da-oct8-2018  
KS\_BIANCu-A2  
PROTON, CDCl3



DA\_OCT26\_2018  
KS-STY6

